Plant Stress 22 (2026) 101480

Contents lists available at ScienceDirect

Plant Stress

journal homepage: www.sciencedirect.com/journal/plant-stress

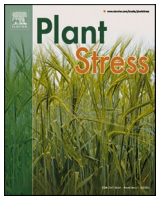

Species-specific BVOC emission dynamics of *Pinus sylvestris* and *Juniperus communis* during different drought intensities

Judith Schmack [a], Anna de Vries [b], Felix Spielmann [b], Jörg-Peter Schnitzler [c,d], Jana Barbro Winkler [c], Baris Weber [c], Georg Wohlfahrt [b], Thomas Karl [a], Werner Jud [a,*]

[a] Department of Atmospheric and Cryospheric Sciences, University of Innsbruck, 6020, Innsbruck, Austria
[b] Department of Ecology, University of Innsbruck, 6020, Innsbruck, Austria
[c] Research Unit Environmental Simulation, Helmholtz Zentrum München, 85764, Neuherberg, Germany
[d] Ecosystem Physiology, Faculty of Environment and Natural Resources, University Freiburg, 79110, Freiburg, Germany

ARTICLE INFO

Keywords:
Scots pine
Common juniper
Alpine conifers
Drought stress
Drought induced BVOCs
Stomatal optimization

ABSTRACT

Climate change is shifting drought frequency and severity in alpine regions, affecting plant physiological processes, including the production and emission of biogenic volatile organic compounds (BVOCs), that influence atmospheric chemistry and the radiative properties of the atmosphere.

While constitutive BVOC emissions are well-characterized for some plant species, drought-induced changes in monoterpene and sesquiterpene emissions remain poorly constrained, limiting predictions for future climate scenarios. We quantified the gas exchange of two conifer species, *Pinus sylvestris* and *Juniperus communis*, in a multi-week plant cuvette experiment with four drought intensity treatments. Continuous gas exchange measurements resolved temporal dynamics of CO_2 assimilation, transpiration, and BVOC emissions. Under severe drought, *P. sylvestris* maintained a positive carbon balance (21.0 g C m^{-2} leaf area), while *J. communis* experienced net carbon loss (-0.48 g C m^{-2} leaf area), reflecting contrasting carbon-uptake versus water-use strategies under drought stress. Total monoterpene emissions were largely drought-insensitive, although our data revealed a compound-specific regulation in *P. sylvestris*. Sesquiterpene emissions were strongly induced in both species, but diverged during the course of the experiment: sustained elevation in *J. communis* versus a bell-shaped response in *P. sylvestris*. Methyl salicylate responses were opposite: stress-induced and unimodal in *P. sylvestris,* but declining with drought severity in *J. communis*.

These findings demonstrate that BVOC drought responses are determined by species-specific carbon balance and physiological thresholds rather than phylogeny alone, providing important insights for models of BVOC emission dynamics under climate change.

1. Introduction

Climate change is expected to alter precipitation patterns worldwide, leading to more frequent and severe summer drought across the Alpine region (e.g., Kotlarski et al., 2023). Drought is a significant abiotic stressor that restricts plant carbon uptake, hydraulic functioning and growth. This has consequences for ecosystem productivity and resilience (e.g., Grant, 2012; Gupta et al., 2020). Water limitation can also restructure plant metabolism and modify the production and emission of biogenic volatile organic compounds (BVOCs) (e.g., Knudsen and Gershenzon, 2020).

BVOCs are a diverse group of chemicals, including oxygenated VOCs and terpenoids, that perform various ecological functions. They mediate interactions among plants and with other organisms, contributing to stress signaling and defense against herbivores and pathogens (Guenther et al., 1995; Baldwin et al., 2006; Dudareva et al., 2006; Duan et al., 2024). Once emitted to the atmosphere, BVOCs are highly reactive trace gases, influencing tropospheric oxidant budgets and the formation of secondary organic aerosol with subsequent effects on air quality, cloud condensation nuclei, and radiative forcing (Fehsenfeld et al., 1992; Bonn and Moortgat, 2002).

Abiotic stress factors like high temperatures or water limitation can induce stress responses in plants through altered BVOC emissions (Holopainen and Gershenzon, 2010; Loreto and Schnitzler, 2010; Seco

* Corresponding author.
E-mail address: werner.jud@uibk.ac.at (W. Jud).

https://doi.org/10.1016/j.stress.2026.101480
Received 13 March 2026; Received in revised form 12 June 2026; Accepted 16 July 2026
Available online 16 July 2026

et al., 2015), suggesting globally changing BVOC emission patterns in a changing climate. These stress responses depend on the type of stress(es) and can vary with duration and severity (e.g., Fortunati et al., 2008; Ferracci et al., 2020; Werner et al., 2021).

Interpreting the mechanisms of drought stress induced BVOC emission changes is challenging, because water shortage influences multiple plant physiological processes simultaneously with opposing effects. Processes that tend to decrease BVOC emissions include reduced carbon assimilation following drought-induced stomatal closure, limiting both BVOC precursor supply and diffusion pathways (Niinemets and Reichstein, 2003; Seco et al., 2015). Conversely, processes that can increase the BVOC release include induced emissions within the stress signaling framework, shifts in enzymatic activity, and ultimately, the loss of tissue integrity (Grant et al., 2012; Kreuzwieser et al., 2021).

BVOC stress responses are further complicated by the existence of multiple emission mechanisms depending on the chemical compound in question, as well as species-specific patterns (Loreto and Schnitzler, 2010).

The lipophilic nature of some BVOCs enables them to cross cellular membranes and be released into the surrounding environment (Dudareva and Pichersky, 2006). Thus, the emission rate is not solely a function of stomatal conductance and the partial pressure gradient between the atmosphere and substomatal cavities, but it is also modulated by compound-specific gas–liquid partitioning and alternative diffusion pathways (Niinemets and Reichstein, 2003; Picherski, 2006).

Generally, two emission mechanism can be distinguished; *de-novo* and storage pool emissions. *De-novo* emissions describe BVOCs that are produced from recently fixed carbon and photosynthetic intermediates, and that are emitted shortly after in a light- and temperature-dependent manner (Tingey, 1980).

Many conifers store large quantities of monoterpenes and sesquiterpenes in specialized structures such as resin ducts (e.g., Ghirardo et al., 2010). Emissions from these storage pools are driven primarily by temperature-dependent volatilization and are largely independent of current metabolic activity (Tingey et al., 1980; Guenther et al., 1991). For *P. sylvestris*, it has been shown that approximately 40−70% of monoterpene emissions may originate from storage pools rather than *de-novo* synthesis (Ghirardo et al., 2010).

While storage-driven emissions are largely governed by physical controls, *de-novo* emissions primarily track constitutive metabolic activity (Tingey et al., 1980; Guenther et al., 1991). In response to abiotic or biotic stress, BVOC emissions from storage pools can act as a passive defense mechanism that is independent of current photosynthetic activity, whereas the release of *de novo*-synthesized BVOCs can serve as an immediate and flexible stress response. These compounds may deter herbivores, attract parasitoids or predators of herbivores, inhibit pathogens, prime defenses in neighboring tissues or nearby plants, stabilize membranes, protect against oxidative stress, and contribute to thermotolerance and ozone detoxification (Loreto and Schnitzler, 2010; Dudareva et al., 2013). The blend of constitutive and stress-induced BVOCs has been shown to differ between plant species and type of stress (e.g., Penuelas and Staudt, 2010; Fitzky et al., 2023).

To explore how these contrasting storage- and *de-novo*-driven BVOC dynamics manifest at the species level and under stress, in the study presented here we focused on the direct comparison of two conifers species commonly found in alpine ecosystems: *Pinus sylvestris* (scots pine) and *Juniperus communis* (common juniper) are widespread species in boreal and temperate ecosystems as well as the Alpine region, often occurring together (Durrant et al., 2016; Enescu et al., 2016). They are also the main species growing in an alpine forest at Mieming, Austria, where the University of Innsbruck operates the multidisciplinary Forest-Atmosphere-Interaction-Research (FAIR) field site (Platter et al., 2024). *Pinus sylvestris* and *J.* communis are well adapted to challenging environmental conditions, including nutrient-poor soils and seasonal droughts. Both species are gymnosperms classified as conifers (*Coniferales*) but belong to different families (*Pinaceae* vs. *Cupressaceae*), thus sharing general gymnosperm characteristics while differing in family-specific traits such as leaf and cone morphology. Their responses to prolonged water stress have been shown to differ in terms of, e.g., stomatal aperture and growth due to species-specific physiological traits (Linton et al., 1998; Weber et al., 2007; Zweifel et al., 2009).

Volatile organic compound emissions from *P. sylvestris* have been examined in several studies, including drought experiments (e.g., Wu et al., 2015; Lüpke et al., 2017; Kreuzwieser et al., 2021), but the effect of prolonged water stress on emission rates and compound composition remains poorly characterized. Additionally, to the best of our knowledge, there exist no systematic and time-resolved studies on the effect of drought on the BVOC emissions of *J. communis*.

In this study, we investigated how drought intensity and duration affect the physiological performance and BVOC emissions of two-year-old *P. sylvestris* and *J. communis* saplings under controlled climatic conditions and four defined water-limitation scenarios ranging from well-watered control plants to severe drought.

We formulated four *a-priori* hypotheses to guide our analysis.

First (H1), we hypothesized that both species would exhibit progressive stomatal closure to minimize water loss, and declining net CO_2 assimilation with increasing drought intensity. However, we expected that distinct strategies for drought tolerance would lead to species-specific stomatal optimization patterns and a decline in photosynthesis at different soil moisture thresholds.

Regarding monoterpene emissions of *P. sylvestris* under drought stress, available literature is somewhat inconclusive. Kreuzwieser et al. (2021) reported unchanged monoterpene emissions under three-week long drought. While Wu et al. (2015) detected increased monoterpene emissions under mild drought, Lüpke et al. (2017) observed substantial reductions under severe 11-day drought. We hypothesized (H2) that monoterpene emissions of *P. sylvestris* from *de-novo* sources would be induced upon mild drought conditions and cease due to a lack of substrate upon severe drought. On the other hand, we hypothesized that monoterpene emissions from storage pools would remain relatively stable across drought treatments, as suggested by Kreuzwieser et al. (2021). Given the contradictory findings across studies differing in drought duration, severity, and plant age, we took an exploratory approach to investigate whether compound-specific monoterpene responses, detectable via Gas Chromatography–Mass Spectrometry (GC–MS), but masked in bulk Proton Transfer Reaction Time-of-Flight Mass Spectrometry (PTR-ToF-MS) measurements, could reconcile these discrepancies. We further investigated whether *J. communis* shows similar compensatory mechanisms to those suggested for *P. sylvestris* (Kreuzwieser et al., 2021) or whether species-specific drought strategies result in divergent emission patterns.

Given that in *P. sylvestris* sesquiterpenes are predominantly synthesized *de-novo* via the cytosolic mevalonic acid (MVA) pathway (Nabeta et al., 1993; Dudareva et al., 2013), we predicted (H3) that their emissions would show progressive weakening under drought as substrate availability and metabolic activity become constrained (Sancho-Knapik et al., 2017). Due to the lack of experimental data of the drought response of *J. communis*, we treated comparative patterns between *P. sylvestris* and *J. communis* as exploratory.

We finally (H4) hypothesized that the emissions of methyl salicylate (MeSA), a stress-signaling compound involved in oxidative stress protection during drought (Filella et al., 2007; Hussain et al., 2019; Singewar et al., 2021), would be induced under moderate drought stress as an adaptive defense response. However, we assumed that with progressing, severe drought, insufficient metabolic carbon availability would eventually lead to declining MeSA emissions.

2. Materials and methods

2.1. Plant preparation

We used two-year-old *P. sylvestris* and *J. communis* saplings, grown at

the Landesforstgarten Bad Häring, Tirol, Austria. They were potted in 2-liter polypropylene pots (Pöppelmann TEKU® Rose Containers 5°, VCE series, Pöppelmann GmbH & Co. KG, Lohne, Germany) that previously had been heated to 60 °C for 22 h to allow VOCs contained in the plastic to evaporate. The soil was a mixture of ¾ commercially available nursery soil ('Patzer Erden Blue Substrate' Type: Blue Container) and ¼ forest soil collected at the FAIR site in Mieming, Austria. The forest soil was included for introducing native mycorrhizal communities. The plants were kept outdoors at the Botanical Garden of the University of Innsbruck under ambient conditions for six weeks.

The trees were then transferred to a chamber of the ExpoSCREEN at the Helmholtz Center Munich in Neuherberg, Germany (Roy et al., 2021), for an acclimatization period of four weeks prior to the experiment. One week before measurements started, irrigation was adjusted to adapt the plants to four different target soil water content levels (see below).

The experimental protocol was conducted sequentially for each species: first *P. sylvestris*, then *J. communis*. During the *P. sylvestris* experiment, *J. communis* plants were kept in the ExpoSCREEN chamber to maintain their acclimatized state. For the actual experiments—measuring assimilation and transpiration rates as well as the VOC exchange—the plants were moved to the VOC-SCREEN facility (Jud et al., 2018) at the Helmholtz Center.

2.2. Drought scenarios

Each experiment included four treatment groups (one well-watered control and three drought levels) with five biological replicates per group ($n = 5$ plants). The target volumetric soil water content (Θ_v) levels were chosen based on soil water retention curves (pF analysis) of the soil mixture (Supplementary Fig. S1) as:

- Control (35% Θ_v, pF 1.8, field capacity)
- Mild Drought (25% Θ_v, pF 2.3),
- Intermediate Drought (15% Θ_v, pF 3.0)
- Severe Drought (10% Θ_v, pF 3.8).

All values were above the permanent wilting point (pF 4.2, Θ_v = 7.5%).

During the *P. sylvestris* experiment, we observed that initial stress levels produced only minimal reductions in net CO_2 assimilation. Therefore, target Θ_v values were progressively reduced from day 21 onwards (final values: Severe 3%, Intermediate 5%, Mild 10%, Control 20%) in order to elicit stronger physiological responses. This extended the gas exchange measurement period for *P. sylvestris* to five weeks instead of four, as was the case for *J. communis*. During the *J. communis* experiment, we aimed to replicate the evolution of Θ_v values described above (starting with the original target soil humidity, progressively decreasing to the adapted target soil water content from day 14 on) for best comparability between the experiments. Actual Θ_v values were continuously monitored using 5TM soil moisture and temperature sensors (Decagon Devices Inc., Pullman, WA, USA; one sensor per pot) and are shown in Supplementary Fig. S2. The plants were typically irrigated every third day. The total water volumes were adjusted to maintain the target average Θ_v per group and were irrigated in two steps with ten minutes in-between, to maximize the water uptake into the soil and to prevent runoff at the sides of very dry soil.

2.3. Experimental setup

The VOC-SCREEN facility at the Helmholtz Center Munich consists of an ExpoSCREEN chamber equipped with 24 custom-built glass cuvettes designed for gas exchange measurements (see Jud et al., 2018, for a detailed description). It allows to continuously monitor air and soil temperature, air humidity and Θ_v in each cuvette.

In our experiment, six cuvettes per treatment group contained five plant-bearing pots, and one soil-only pot. The latter was used as reference to measure the background signals, e.g., VOC emissions from the soil/pot and instrument background. Assimilation and transpiration rates, as well as VOC exchange were measured sequentially (5 min per plant cuvette, 10 min per background cuvette, 140 min for all cuvettes).

Chamber conditions simulated a typical mid-summer diurnal cycle based on measurements at the FAIR site (Mieming, Tirol, Austria) during June–August 2023 (for detailed description of climatic conditions, see de Vries et al., 2026). Temperature and humidity inside the cuvettes were continuously monitored with combined air temperature and humidity sensors (model DKRF400, Driesen + Kern GmbH, Bad Bramstedt, Germany). Cuvette temperature ranged from 17 ± 1.0 °C at night to 27 ± 1.2 °C during the day. Relative humidity ranged from 38 ± 9% during the day to 75 ± 2% at night.

Photosynthetically active radiation was provided by the phytotron's lighting system following a simulated natural photoperiod: lights activated at 04:00 UTC, ramping to a maximum photosynthetic photon flux density (*PPFD*) of 700 µmol m^{-2} s^{-1} at 09:00 UTC (maintained for 7 h), then gradually decreasing until lights-off at 20:00 UTC (16 h photoperiod).

Cuvette inlet flow rates were set to 6 slm (standard liters per minute) for *J. communis* (all treatments) and the Severe Drought group of *P. sylvestris*, and 7 slm for the Control, Mild, and Intermediate Drought groups of *P. sylvestris*. Higher flow rates avoided condensation in cuvettes containing highly transpiring plants. These flow rates corresponded to cuvette air residence times of approximately 6.7 min and 5.7 min, respectively. Cuvette-specific inlet flow rates were considered accordingly in the gas exchange calculations (cf. Sections 2.6 and 2.9).

Air exiting the cuvettes was split between several measuring devices as follows:

- 80 sccm (standard cubic centimeters per minute) to GC–MS sampling tubes (Tenax + Carbopack™ filled; twice a week)
- 500 sccm to a quantum cascade laser measuring COS (de Vries et al., 2026)
- 500 sccm to an infrared gas analyzer (IRGA, model LI-840A, LI-COR, Lincoln, NE, USA) for CO_2 and H_2O measurement
- 3.5 slm to a PTR-ToF-MS for continuous BVOC analysis. The model used in this experiment was the PTR-ToF-MS 6000×2 (Ionicon Analytik GmbH, Innsbruck, Austria).

The difference between the cuvette inlet and outlet flow (~1.4 slm or 2.4 slm for an inlet flow rate of 6 slm and 7 slm, respectively) assured a slight overpressure inside the cuvettes, preventing chamber air entering the cuvettes through inevitable leaks. Due to the malfunctioning of the watering system in one of the cuvettes and subsequent death of the plants inside, this cuvette (no. 10; severe drought treatment for *P. sylvestris* experiment, intermediate drought treatment for *J. communis* experiment) was excluded from further analyses for both experiments.

2.4. GC–MS analyses

Twice a week, targeted VOC measurements were conducted using GC–MS to distinguish isomeric compounds (e.g., individual monoterpene and sesquiterpene species) that cannot be resolved by PTR-ToF-MS. VOCs were collected using sorbent tubes filled with Tenax/Carbopack™ (40 mg Tenax TA 60/80 and 60 mg Carbopack™ X 40/60, Sigma-Aldrich, St. Louis, USA) at a flow rate of 80 sccm for 7 h during peak daylight hours. Before sampling, each tube was spiked with 2 µl of δ−2-carene (429.7 pmol μL^{-1} solved in methanol) as an internal standard.

The sampling tubes were then analyzed with a GC–MS (GC: 7890A; MSD: 5975C Agilent Technologies, Palo Alto, CA, USA) equipped with a thermo-desorption unit (Gerstel GmbH, Mülheim an der Ruhr, Germany).

Sampled VOCs were thermally desorbed by heating from 30 °C to

270 °C at a rate of 280 °C min^{-1}, followed by a 12 s hold. In the next step, the sampled VOCs were cryo-focused on a Tenax TA liner at −50 °C for 18.6 s, followed by rapid heating to 270 °C at 12 °C s^{-1} (2 min hold) for a second desorbing. The GC temperature ramp started at 40 °C, then increased at a rate of 8 °C min^{-1} to 130 °C (hold for 5 min), followed by 80 °C min^{-1} to 175 °C, 2 °C min^{-1} to 200 °C, 4 °C min^{-1} to 220 °C, and finally at 100 °C min^{-1} to 300 °C (hold for 5 min). Chromatographic separation was achieved using a (14%-Cyanopropyl-phenyl)- methylpolysiloxane GC column (DB-5MS 10 m DG, 69 m × 250 µm × 0.25 µm, Agilent Technologies).

Volatile organic compounds were identified using the software ChemStation (Agilent Technologies, USA) by comparing the mass spectra with the NIST20 library (National Institute of Standards and Technology, Gaithersburg, Maryland, USA).

For VOC quantification, calibration curves based on pure standards of α-pinene, β-pinene, eucalyptol, linalool, methyl salicylate, bornylacetate, β-caryophyllene, α-humulene (Carl Roth, Karlsruhe, Germany; Sigma Aldrich, Deisenhofen, Germany) at six different concentrations from 55 to 800 pmol μL^{-1} each, were used. All extracted VOC data are based on the Extracted Ion Chromatogram (EIC) signal and are normalized to the internal standard δ−2-carene (859.3 pmol μL^{-1}) of each measurement. After quantification, the measured BVOC concentrations of the background cuvettes (containing soil-only pots) were subtracted from the BVOC concentrations of the plant cuvettes. Plant-wise mean VOC fluxes over the GC sampling period were obtained by normalizing the VOC concentrations to the plant leaf area and the cuvette inlet flow rate.

Differences between the Control group and each drought group were tested independently for each sampling day using two-sided Mann-Whitney U tests. Significance is indicated as: * $p < 0.1$, ** $p < 0.05$, *** $p < 0.01$.

2.5. Leaf area and leaf temperature calculation

Leaf area was determined post-experiment using a subsampling approach: needles were scanned to measure their projected area, then dried and weighed to determine the specific leaf area (cm^2 g^{-1} dry weight). The projected leaf area of all needles of the individual plants was calculated from this ratio and the dry weight of all their needles. This projected leaf area was used to calculate all fluxes.

To estimate temporal changes in projected leaf area (due to growth and senescence), each plant was photographed before and after the experiment with two cameras positioned at 0° (front) and 45° angles while the plant was rotated to seven positions on a rotating plate, resulting in 14 images per plant. Leaf area changes were assumed to be linear throughout the experiment and interpolated accordingly. While this approach introduces some uncertainty in temporal leaf area estimates, it avoided removing plants for non-destructive leaf area determination from cuvettes during the experiment, which would have induced wound-related VOC emissions and disrupted measurements. We recognize that the assumption of linear leaf area change is a simplification that may not fully capture the actual leaf area dynamics.

Leaf temperature (T_{leaf}), used for the calculation of vapor pressure deficit (VPD) and stomatal conductance, was not directly measured but estimated from air temperature (T_{air}) with treatment-specific offsets. Well-watered conifers maintain needle temperatures close to air temperature through evaporative cooling, while drought-stressed plants experience elevated leaf temperatures (Muller et al., 2021). Based on literature values showing needle warming of 1–3 °C under moderate to severe drought in pines (Seidel et al., 2016; Muller et al., 2021), we applied corrections: $T_{leaf} = T_{air}$ for Control and Mild drought, $T_{leaf} = T_{air} + 1$ °C for Intermediate drought, and $T_{leaf} = T_{air} + 2$ °C for Severe drought. Please note that this conservative correction might still not fully capture the actual leaf temperature and associated dynamics. We assume the remaining error to be <2 °C.

2.6. Calculation of CO_2 and H_2O exchange

Transpiration rate (E) and CO_2 assimilation rate (A) were calculated from water vapor and CO_2 concentrations measured at the cuvette inlet and outlet using two non-dispersive infrared gas analyzers (IRGA, model LI-840A, LI-COR Biosciences, Lincoln, Nebraska) following von Caemmerer and Farquhar (1981):

$$E = \frac{u_e}{A_{leaf}} \times \frac{w_o - w_e}{1 - w_o \times 10^{-3}} \quad (1)$$

$$A = \frac{u_e}{A_{leaf}} \times \left[c_e - \left(\frac{1 - w_e \times 10^{-3}}{1 - w_o \times 10^{-3}} \right) \times c_o \right] \quad (2)$$

where u_e is the molar flow rate of air entering the cuvette (mol s^{-1}), A_{leaf} is leaf area (m^2), w_e and w_o are the mole fractions of water vapor entering and exiting the cuvette (mmol mol^{-1}), and c_e and c_o are the mole fractions of CO_2 entering and exiting the cuvette (µmol mol^{-1}).

To assess total productivity, cumulative net carbon gain was calculated for each plant by integrating assimilation rates over the entire experiment duration using trapezoidal integration. To this end, net assimilation (A) was multiplied by −1 to get positive values in the case of CO_2 fixation. Carbon exchange in form of BVOC was not considered here, as these compounds made up only a small fraction of the total carbon balance.

Treatment effects on cumulative carbon gain were assessed using one-way analysis of variance (ANOVA) with treatment as a fixed factor and individual plants as replicates ($n = 5$ per treatment, except $n = 4$ for the Severe treatment of *P. sylvestris* and the Intermediate treatment of *J. communis*, see above). Statistical significance was set at $\alpha = 0.05$. Results are reported as F-statistics with degrees of freedom ($F_{df1,df2}$) with df1 representing the degrees of freedom between groups (number of groups minus one) and df2 representing the degrees of freedom within groups (total number of tested plants minus number of treatments).

For time-series visualization of cumulative carbon gain, treatment-group means were calculated at each time point, with variability displayed as standard error (SE).

2.7. Calculation of stomatal conductance and Medlyn stomatal optimization theory

Stomatal conductance to water vapor ($g_{s,\ H_2O}$) was calculated from the transpiration rate and vapor pressure deficit (*VPD*) (Farquhar and Sharkey, 1982):

$$g_{s,\ H_2O} = \frac{E \times p}{VPD} \quad (3)$$

where E is the transpiration rate (mol m^{-2} s^{-1}), p is atmospheric pressure (assumed constant at 100 kPa), and *VPD* is vapor pressure deficit (kPa) calculated from leaf temperature and relative humidity using the Tetens equation (Tetens, 1930).

Stomatal conductance to CO_2 (g_s, mol m^{-2} s^{-1}) was then calculated using the standard diffusivity ratio (von Caemmerer and Farquhar, 1981):

$$g_s = \frac{g_{s,\ H_2O}}{1.6} \quad (4)$$

To characterize stomatal behavior and water use efficiency strategies across drought treatments, we fitted the unified stomatal optimization model of Medlyn et al. (2011). This model provides a theoretically grounded framework for linking stomatal behavior to carbon-water economics and has been widely investigated across plant functional types (e.g., Lin et al., 2015). It is based on the expression of stomatal conductance as:

$$g_{s,\ H_2O} = g_0 + 1.6\left(1 + \frac{g_1}{\sqrt{VPD}}\right)\frac{A}{C_a} \quad (5)$$

from Medlyn et al. (2011) and the provided corrigendum (Medlyn et al., 2012). g_0 is here the baseline stomatal conductance to water vapor (mol H_2O m^{-2} s^{-1}), g_1 is the stomatal slope parameter ($\sqrt{kPa}$) representing the plant's water use efficiency strategy, A is net CO_2 assimilation rate (µmol CO_2 m^{-2} s^{-1}), and c_a is ambient CO_2 concentration (µmol mol^{-1}, measured at cuvette outlet).

Data for the Medlyn model approach were filtered prior to model fitting according to the following criteria to ensure robust parameter estimation: (1) daytime periods where $PPFD > 100$ µmol m^{-2} s^{-1}, (2) $VPD > 1.0$ kPa to avoid low VPD conditions where stomatal responses are poorly constrained, (3) valid (non-NaN, finite) values of g_s and the predictor term $A/(c_a \times \sqrt{VPD})$, and (4) net CO_2 uptake rates ($A < -0.1$).

Following Lin et al. (2015), we constrained $g_0 = 0$ to force the regression fit through the origin. For more details on why this simplification is justified, see Lin et al. (2015).

To minimize the effect of outliers on the model parameter estimation, we employed RANSAC (Random Sample Consensus) robust regression, a nonlinear iterative algorithm that identifies and excludes outliers (Fischler and Bolles, 1981). The RANSAC algorithm was implemented in Python using scikit-learn with a linear regression base. The parameter g_1 was derived from the regression slope. Fitted relationships were visualized using hexagonal binning density plots to illustrate data distribution and model fit quality. Model performance was assessed using the coefficient of determination (R^2) calculated on the full dataset to maintain comparability across treatments.

Uncertainty in g_1 was quantified using bootstrap resampling with 1000 iterations (sampling with replacement), where RANSAC regression was applied to each resampled dataset. The 95% confidence interval was derived from the 2.5th and 97.5th percentiles of the resulting bootstraped distribution.

2.8. Selection of target VOCs

To identify VOCs exhibiting drought-responsive emission patterns, we visually screened all signals detected with PTR-ToF-MS for diurnal emission cycles characteristic of plant-derived compounds. This resulted in a list of a few dozens of mass-to-charge ratios (m/z, with $z = 1$) in both experiments (see Supplementary Tables S1 and S2). We then selected the compounds that responded most strongly to drought stress for a detailed temporal analysis.

For an in-depth analysis, we focused on three compound classes that met multiple selection criteria. Monoterpenes (in PTR-ToF-MS detected at m/z 137.133 + fragments at m/z 81.070, with no apparent interference from hexenal fragments at m/z 81.070) and sesquiterpenes (m/z 205.196 + fragments at m/z163.149, m/z 161.133, m/z 149.133, m/z 135.116, m/z 123.117, m/z 109.102) exhibited the strongest drought-related emission changes in preliminary group-wise comparisons. They are among the most prominent BVOC emissions from conifers (e.g., Guenther et al., 2012) and are of central importance for understanding *de-novo* biosynthesis versus storage pool contributions under stress (Ghirardo et al., 2010; Niinemets et al., 2010). Methyl salicylate (m/z 153.055), though emitted at lower rates, in our experiments showed clear species- and treatment-dependent emission patterns. It is known as a marker of stress-induced defense signaling (Filella et al., 2007) and was thus also selected for an in-depth analysis. These three compound classes were additionally confirmed and specified by targeted GC–MS measurements (see above), providing further insight into drought-induced emission changes.

For *P. sylvestris* and *J. communis* we were able to identify 61 and 65 VOCs, respectively, using GC–MS (see Supplementary Tables S3 and S4 for a complete list). Only the emission rates of five VOCs that displayed pronounced differences between the drought groups and contributed to the analysis of our PTR-ToF-MS measurements are shown.

2.9. VOC-Flux calculation

VOC fluxes were calculated from PTR-ToF-MS data as follows: raw data were processed using IoniTOF Data Analyzer v2.2.0.3 (Ionicon Analytik GmbH, Innsbruck, Austria) to obtain count rates (counts per second, cps) for detected mass-to-charge ratios. The results were further post-processed with custom routines to obtain concentration data. Eventually, VOC fluxes were calculated following the method described in Jud et al. (2018), with the net plant emission rate e_i being calculated as

$$e_i = \frac{F_{in}}{A_{leaf}} \times \left(c_{i,cuvette} - c_{i,\ BG}\right) \quad (6)$$

where F_{in} is the cuvette inlet flow rate (m^3 s^{-1}), A_{leaf} is the leaf area (m^2), $c_{i,cuvette}$ is the molar concentration (in units of nmol m^{-3}) of compound i measured at the outlet of the plant cuvette, and $c_{i,BG}$ is the molar concentration measured at the outlet of the background (soil-only) cuvette. These concentrations are assumed to be representative of the concentrations within the cuvettes assuming good turbulent air mixing.

We verified that the use of wet vs. dry mole fractions for VOC concentrations had a negligible impact on calculated emission rates. Correction factors calculated from measured relative humidity ranged from 1.0005 to 1.0022 across treatment groups, corresponding to < 0.25% increase in emission rates, which is well within measurement uncertainty.

Parent ion and known fragment ion signals were summed to obtain total compound fluxes. For monoterpenes and sesquiterpenes, fragmentation ratios were determined from the slope of linear regressions of background-corrected fragment ion vs. parent ion signals.

Most analyses were performed at the treatment-group level to examine temporal emission dynamics and to ensure robust statistical power by providing five biological replicates per group.

To isolate the direct effect of soil moisture on BVOC emissions (independent of temporal trends), we analyzed the relationship between emission rates and measured Θ_v. For this analysis, we used only data from peak illumination periods on days when plants were irrigated in the evening, ensuring soil moisture was closest to target values and minimizing transient post-irrigation effects.

3. Results

3.1. CO_2-Uptake and stomatal optimization

Over five (four) weeks of induced drought, *P. sylvestris* and *J. communis* showed distinct physiological responses. Cumulative net carbon gain differed significantly among treatments in both species (Fig. 1). In *P. sylvestris* (36-day experiment, Fig. 1a), Control plants accumulated 65.76 ± 2.52 g C m^{-2} (mean ± SE), while Severe drought plants accumulated 21.20 ± 2.38 g C m^{-2} (60% reduction; $F_{3,15} = 17.2$, $p < 0.0001$). Notably, Mild drought plants showed enhanced productivity (75.64 ± 9.78 g C m^{-2}), though high individual variability rendered this 15% increase non-significant compared to Control ($p = 0.644$). All *P. sylvestris* plants maintained positive carbon balance even under Severe drought.

In contrast, *J. communis* (27-day experiment, Fig. 1b) exhibited more severe drought impacts. Control plants accumulated 19.11 ± 2.04 g C m^{-2}, declining progressively through Mild (6.17 ± 5.80 g C m^{-2}) and Intermediate (5.17 ± 0.35 g C m^{-2}) to Severe drought, where plants eventually experienced net carbon loss (−0.48 ± 0.91 g C m^{-2}; $F_{3,13} = 5.8$, $p = 0.0075$), indicating respiratory carbon consumption exceeded photosynthetic carbon gain. A high individual variability in net carbon gain was observed in the Mild drought group (range: −5.43 to +27.00 g C m^{-2}), with two replicates showing net carbon gain, two replicates showing net carbon loss and one replicate showing negligible net carbon gain.

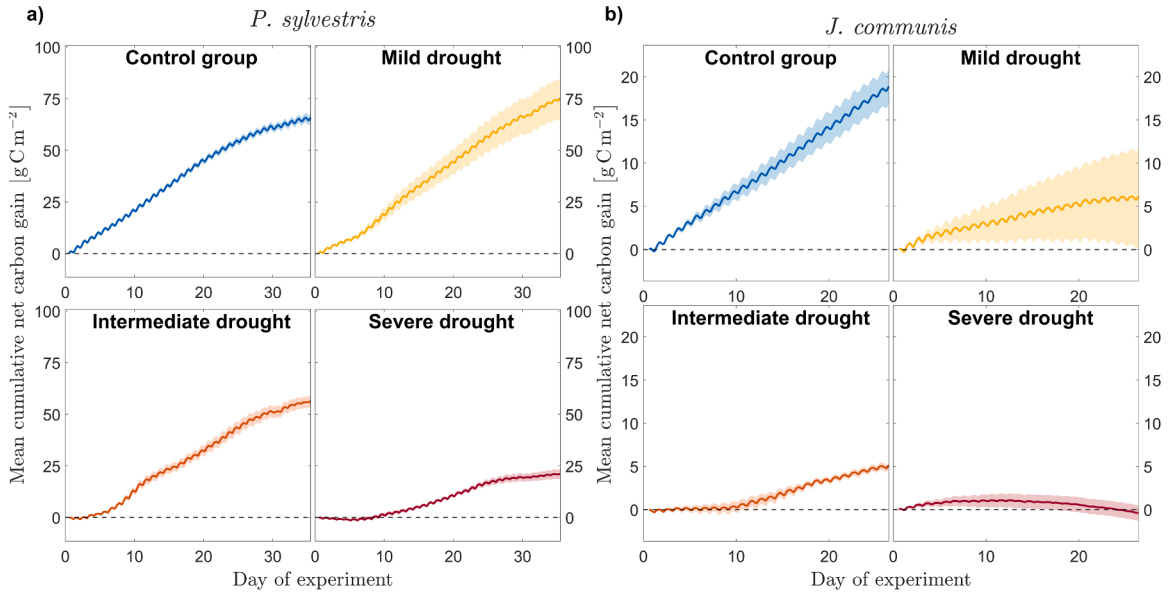

Fig. 1. Average cumulative net carbon gain in a) the P. sylvestris experiment and b) the J. communis experiment. The four panels show the four investigated treatments, respectively. The colored shadings illustrate one standard error (SE). Please note the different *x* and *y* axes scaling between panel (a) and (b).

In order to get a quantitative measure for the species-specific drought tolerance strategies, we fitted the Medlyn stomatal optimization model (cf. Section 2.7) to daytime gas exchange data for each treatment, using RANSAC robust regression (Fig. 2).

For well-watered Control plants of *P. sylvestris* (Fig. 2a), the model yielded a poor fit ($R^2 = -0.403$), with the stomatal slope parameter $g_1 = 4.00$. The stomatal slope parameter declined progressively with drought severity from Mild ($g_1 = 3.11$; $R^2 = 0.574$), through Intermediate ($g_1 = 1.81$; $R^2 = 0.496$) to Severe drought ($g_1 = 0.71$; $R^2 = 0.465$), indicating a shift towards more conservative water use strategies.

In the Control treatment of *J. communis* (Fig. 2b), we obtained a stomatal slope parameter $g_1 = 4.32$ ($R^2 = 0.094$). Under Mild drought, the stomatal slope parameter peaked with $g_1 = 4.35$ ($R^2 = -0.285$) and declined through Intermediate ($g_1 = 2.31$; $R^2 = 0.217$) to Severe drought ($g_1 = 0.71$; $R^2 = 0.465$).

3.2. BVOC Emissions in relation to volumetric soil water content

Drought treatments had a distinct impact on the emissions of several BVOCS. Fig. 3 illustrates the relationship between monoterpene, sesquiterpene and MeSA emission rates, and the volumetric soil water content for both plant species.

Monoterpenes dominated total BVOC emissions in both species and showed minimal dependence on soil moisture (Fig. 3a, b). Emission rates remained relatively constant across the entire Θ_v range, averaging at ~0.25 nmol m^{-2} s^{-1} in *P. sylvestris* and at ~0.02 nmol m^{-2} s^{-1} in *J. communis*.

Methyl salicylate emissions exhibited markedly different responses to soil moisture between species (Fig. 3c, d). In *P. sylvestris*, MeSA emissions displayed a weak unimodal relationship with Θ_v with peak emissions (~0.15 nmol m^{-2} s^{-1}) occurring at soil moisture values of 5–10 %. Emissions declined under both well-watered conditions ($\Theta_v > 30$ %) and severe drought ($\Theta_v < 5$ %).

In contrast, *J. communis* showed a positive relationship between MeSA emissions and Θ_v (Fig. 3d), with lowest emissions under severe drought (~0.0002 nmol m^{-2} s^{-1}) and highest under well-watered conditions (~0.0015 nmol m^{-2} s^{-1}). Notably, MeSA emissions from *P. sylvestris* were ~100-fold higher than from *J. communis* at comparable Θ_v, indicating substantial differences in stress signaling strategies.

Sesquiterpenes appeared to show drought-induced emission patterns in both species, with higher emission rates at lower Θ_v (Fig. 3e, f).

In *P. sylvestris*, maximum sesquiterpene emissions (~0.4–0.8 nmol m^{-2} s^{-1}) occurred at the transition from Intermediate to Severe drought ($\Theta_v = 5$–15%), rather than at the driest conditions.

J. communis exhibited peak sesquiterpene emissions (~0.1 nmol m^{-2} s^{-1}) at the lowest Θ_v values (< 5 %), with emissions declining significantly toward well-watered conditions.

3.3. Temporal dynamics of BVOC emission rates with prolonged drought stress

Daily emission cycles were evident in the PTR-ToF-MS data of all the VOCs examined in more detail (monoterpenes, MeSA, and sesquiterpenes, see Fig. 4), reflecting their strong dependence on photosynthetic activity and/or temperature. There are clear differences observable for the daily cycles of emission rates of these compounds between the two species:

After a very clear monoterpene peak at the beginning of the experiment, likely caused by mechanical damage during the installation of the plants into the cuvettes, *P. sylvestris* (Fig. 4a) reached a phase of stable emission amplitudes with mean values of 0.1 nmol m^{-2} s^{-1} to 0.5 nmol m^{-2} s^{-1}, that did not differ between the drought scenarios. The severe drought group showed a slight rise of emissions at the end of the experiment that correlated with increasing green leaf volatile (GLV) and acetaldehyde emissions (Supplementary Fig. S4c, e).

J. communis displayed more distinct daily cycles in monoterpene emissions than *P. sylvestris* (Fig. 4b), but also did not show any drought related differences. Minimum emissions at night were close to 0 nmol m^{-2} s^{-1}, maximum emissions during daylight conditions reached amplitudes of 0.05 nmol m^{-2} s^{-1} at the start of the experiment, that decreased to around 0.025 nmol m^{-2} s^{-1} towards the end of the experiment. Note that during the whole experiment, *P. sylvestris* emitted about ten times more monoterpenes than *J. communis* (~0.25 vs. 0.025 nmol m^{-2} s^{-1}).

For *P. sylvestris*, MeSA emissions followed a bell-shaped temporal pattern with the highest fluxes peaking at 0.10–0.15 nmol m^{-2} s^{-1} in Intermediate drought around days 15–20 of the experiment (Fig. 4c), before declining again.

In contrast, *J. communis* generally exhibited low MeSA emissions (< 0.001 nmol m^{-2} s^{-1}; Fig. 4d), with the highest daily amplitudes in the

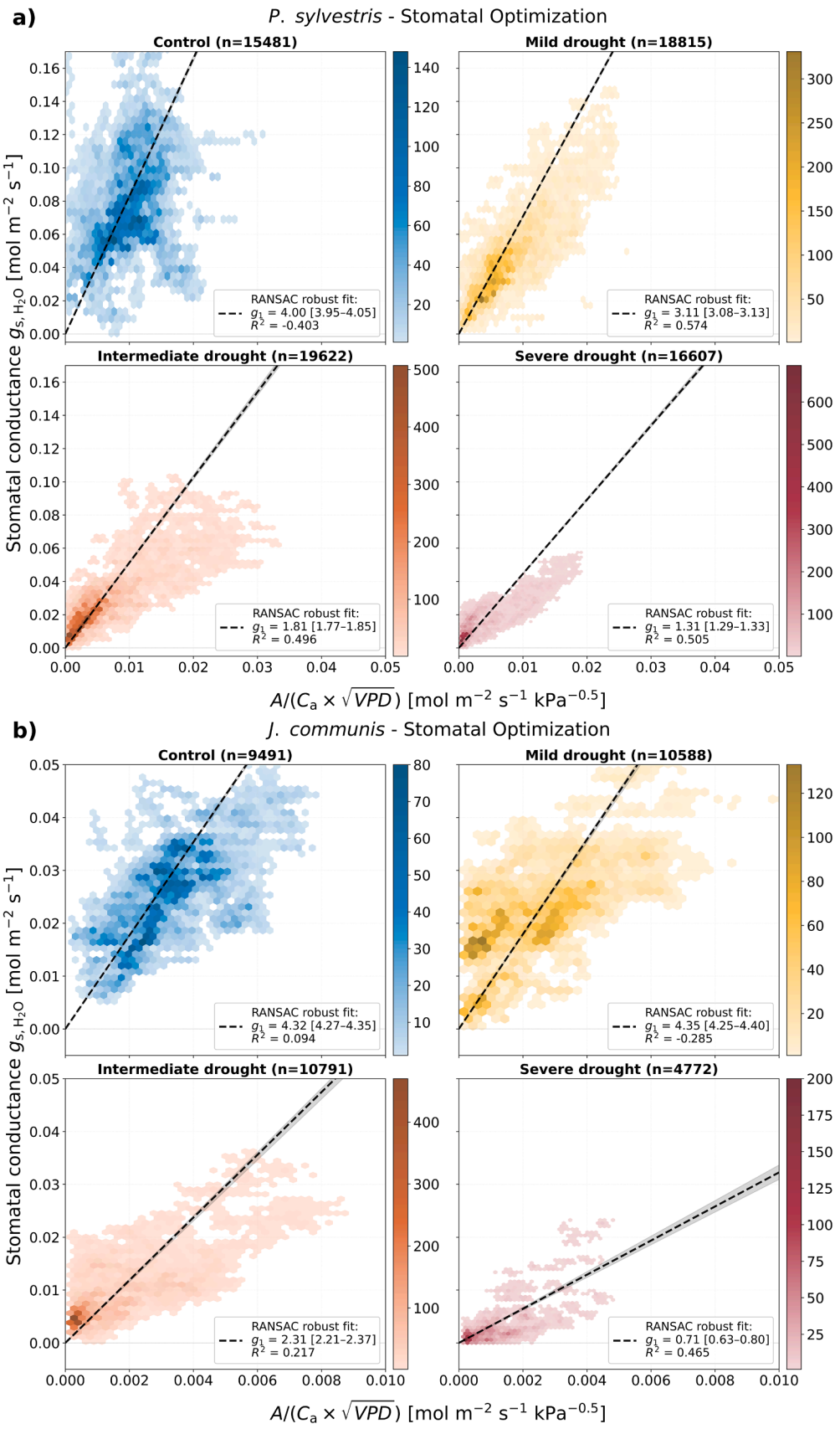

(caption on next page)

Fig. 2. Medlyn stomatal optimization model responses to drought: Stomatal conductance (g_s) as a function of $A/(C_a \times \sqrt{VPD})$ with assimilation (A), ambient CO_2 concentration (C_a) and vapor pressure deficit (VPD) for (a) P. sylvestris and (b) J. communis across Control, Mild, Intermediate, and Severe drought treatments. Dashed lines show treatment-specific robust fits of the Medlyn model. Estimated stomatal slope parameters (g_1) with 95% confidence intervals and coefficients of determination (R^2) are given in the legends, the sample size (n) is given in the subplot headings. The color bars and corresponding shadings show the respective density distribution of points in each panel.

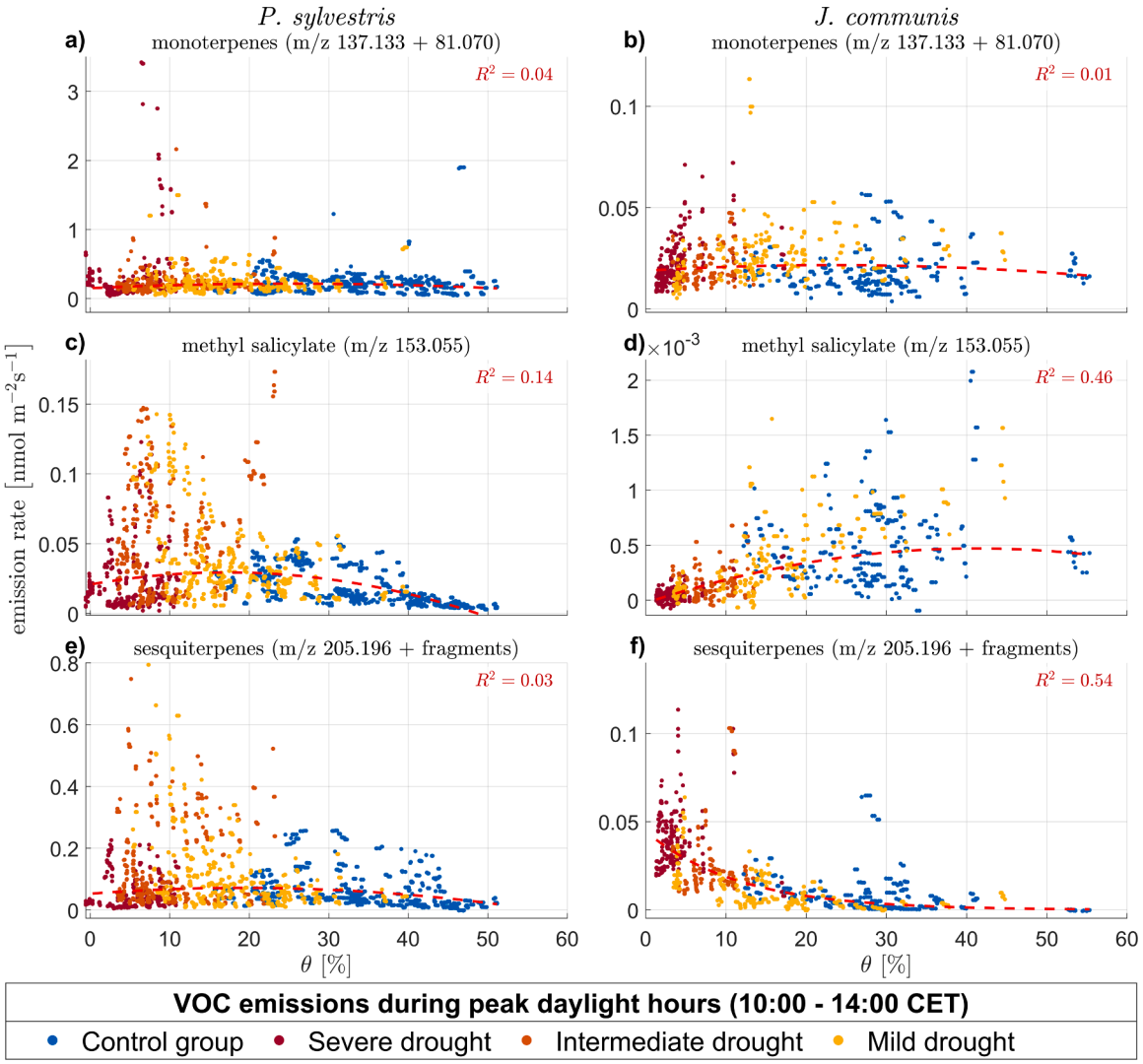

Fig. 3. Emission rates of the most prominent VOCs detected with PTR-ToF-MS as a function of Θ_v. a) and b) monoterpenes, c) and d) Methyl Salicylate (MeSA), e) and f) sesquiterpenes from P. sylvestris (left) and J. communis (right), respectively. Each dot represents one measurement taken at the respective Θ_v during peak daylight hours (10:00 UTC to 14:00 UTC on the day of irrigation, i.e., before each irrigation event). Dashed red lines indicate quadratic fits for each compound group to illustrate overall trends. Respective R^2 values are given in the top right corner. Please note the different y-axis scales in the different panels.

Control group, followed by the Mild drought, and almost no emissions in the Intermediate and Severe drought group. Emission rates declined over the course of the experiment from about 0.001 nmol m^{-2} s^{-1} in the beginning of the experiment to approx. 0.0003 nmol m^{-2} s^{-1} during the last experiment days. In a single plant cuvette of the Mild group, we observed a strong MeSA signal on days 10 to 11. This high signal cannot be attributed to any external cause and remains unexplained.

For the sesquiterpene emissions of the severely stressed group in the *P. sylvestris* experiment (Fig. 4e), a bell-shaped temporal response, similar to that of the MeSA emissions, was apparent, with maximum values of 0.02 nmol m^{-2} s^{-1} at day 20 of the experiment. The Intermediate drought group maintained higher emission rates than the Severe group (around 0.25 nmol m^{-2} s^{-1}) during the whole period and kept these values towards the end of the experiment. The Mild and Control groups initially showed low sesquiterpene emissions but higher ones later on, with the Mild group eventually even surpassing the Intermediate group.

Sesquiterpene emissions from *J. communis* (Fig. 4f) displayed a clear gradient across treatments, increasing from the Control group to the Mild, Intermediate, and Severe drought stressed groups (0.008–0.045 nmol m^{-2} s^{-1} during peak daylight conditions). This pattern was evident from the start of the experiment and became more pronounced over time, since the Control, Mild and Intermediate drought group lowered their emissions towards the end of the experiment. Notably, the Severe drought group showed elevated nighttime emissions of 0.025 nmol m^{-2} s^{-1} in addition to enhanced daytime peaks.

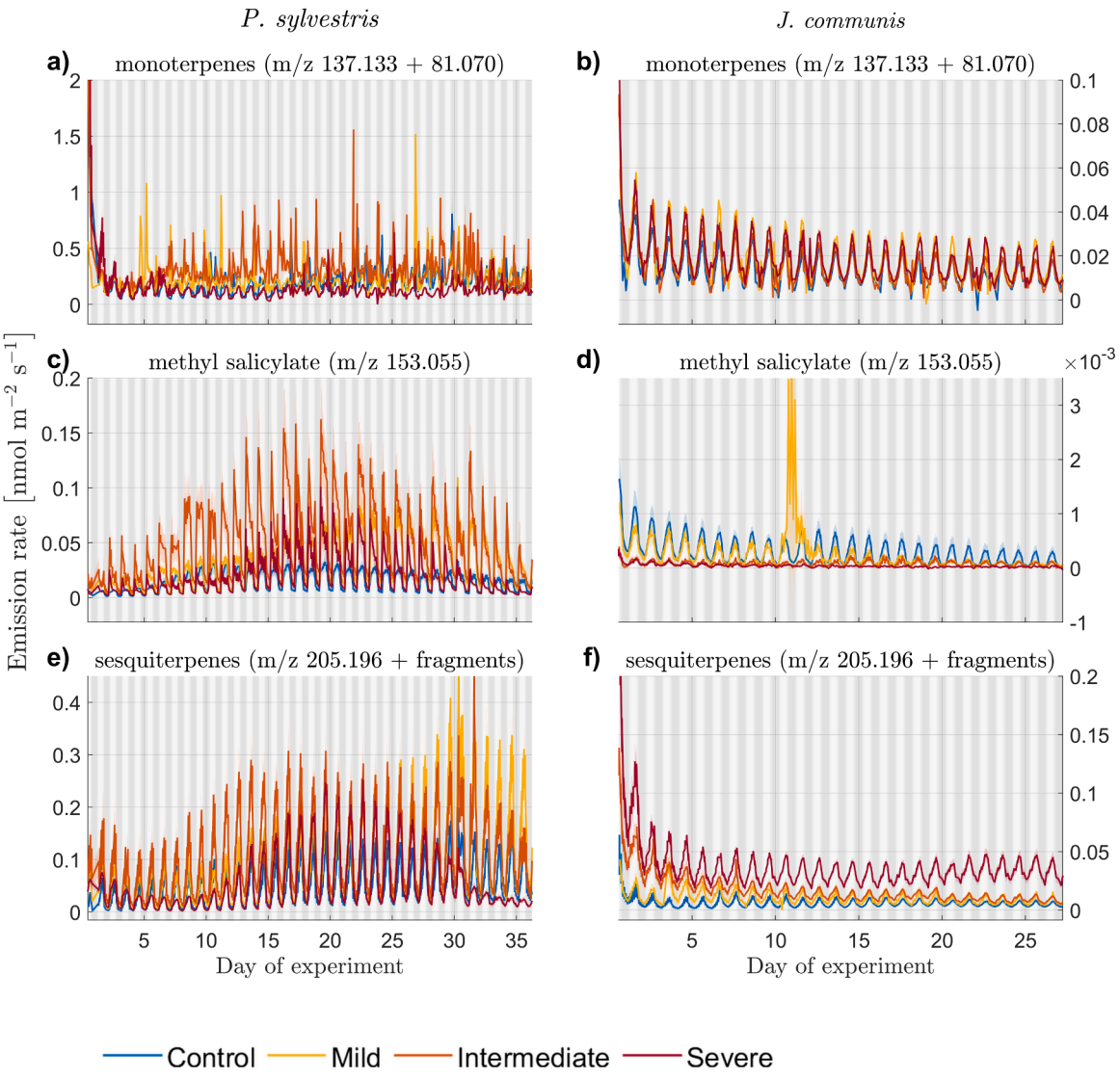

Fig. 4. Emission rates of selected VOCs over the whole experiment duration for a) and b): monoterpenes, c) and d) Methyl Salicylate (MeSA), e) and f): sesquiterpenes from P. sylvestris (left panels) and J. communis (right panels), respectively. The colored lines represent the mean VOC emission rates in the different treatments and the colored, shaded areas the respective standard error. Grey areas indicate periods when the light was turned off. Please note the different scaling of the *y* axes in the individual panes. (For interpretation of the references to color in this figure legend, the reader is referred to the web version of this article.).

3.4. VOC speciation by GC–MS

Since the PTR-ToF-MS cannot distinguish between different compounds detected at the same ion mass, we used complementary GC–MS sampling to separate isomeric VOCs (i.e., mostly mono- and sesquiterpenes). Fig. 5 presents temporal dynamics of individual monoterpene and sesquiterpene compounds, identified by GC–MS analysis in *P. sylvestris*. The box plots illustrate the mean emission rates of several VOCs over seven hours for each treatment ($n = 4$ in the Severe drought treatment, $n = 5$ otherwise) on eight different days throughout the 36-day experiment.

While the PTR-ToF-MS data obtained from *P. sylvestris* showed no clear treatment effects with respect to the summed monoterpene emissions (Figs. 3a and 4a), the compound speciation of GC–MS revealed distinct, although statistically not significant, responses of individual monoterpenes.

Sabinene and D-limonene exhibited opposite relationships with drought stress (Fig. 5a, b). D-limonene emission rates were consistently higher in plants exposed to drought-stress, with plants under Severe and Intermediate drought emitting more than Control plants throughout the experiment (Severe/Intermediate medians: 0.5–1 × 10^{-4} nmol m^{-2} s^{-1}; Control medians: 0.2–0.4 × 10^{-4} nmol m^{-2} s^{-1}; Fig. 5a). This enhancement was particularly evident during the early experiment (days 4–16). All treatments showed declining D-limonene emissions over time, but the relative drought enhancement persisted.

In stark contrast, sabinene emission rates were consistently lower in Severe drought plants (medians: 0.0–0.3 × 10^{-4} nmol m^{-2} s^{-1}) compared to Control plants (medians: 0.3–0.65 × 10^{-4} nmol m^{-2} s^{-1}), indicating suppression at multiple time points (Fig. 5b).

α-farnesene ($C_{15}H_{24}$) was the most abundant sesquiterpene detected, with median emission rates reaching 1.5–2.5 × 10^{-3} nmol m^{-2} s^{-1} in drought-stressed plants (Fig. 5c). Emission rates showed clear drought induction, with Intermediate and Severe treatments exhibiting significantly higher emissions than Control from day 16 onwards. Peak emissions occurred during the mid-to-late experiment period (days 16–33), with particularly high values in the Severe treatment around day 19 (median ~2.2 × 10^{-3} nmol m^{-2} s^{-1}). Within-treatment variability was substantial, especially in drought-stressed groups, as indicated by large interquartile ranges and whisker lengths. Control and Mild drought treatments maintained relatively stable, low α-farnesene emission rates

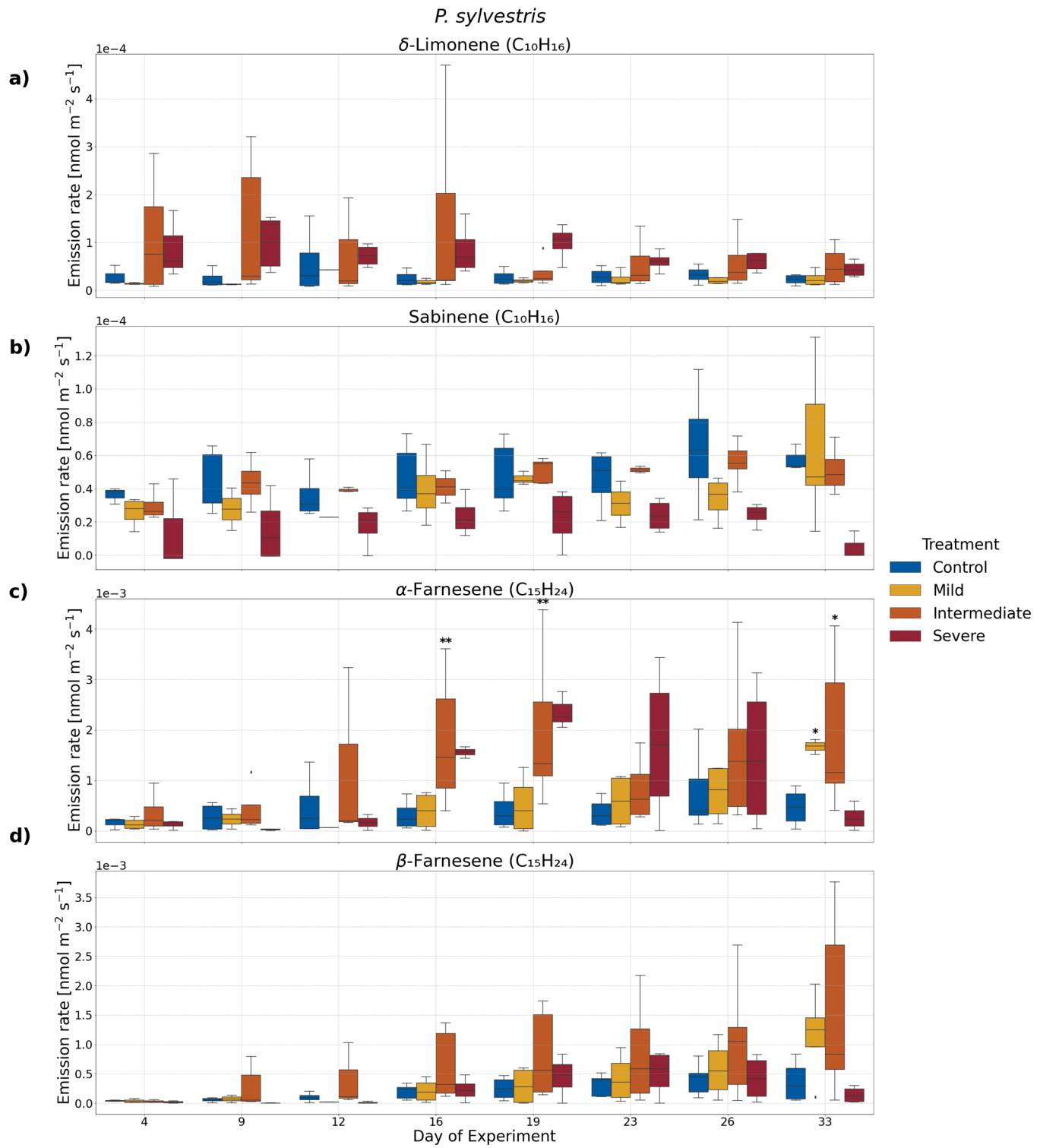

Fig. 5. Mean emission rates of selected BVOCs from Pinus sylvestris in the four treatments, determined for a 7 h light period about every 3rd day with GC–MS. The boxplots illustrate the median emission rates, the interquartile ranges and whiskers extending to 1.5 times the interquartile range. Please note the different scaling of the *y* axes in the individual panes. Stars indicate significant differences between the drought groups and the control group. Significance levels are: * $p < 0.05$, ** $p < 0.01$, *** $p < 0.001$.

(0.2–0.5 × 10^{-3} nmol m^{-2} s^{-1}) throughout the experiment.

β-farnesene ($C_{15}H_{24}$) showed similar drought-induced patterns, but with lower emission rates (0.0–1.3 × 10^{-3} nmol m^{-2} s^{-1} maximum; Fig. 5d) and less days with highly significant differences between the drought groups. Drought induction was evident from day 16, with Intermediate and Severe treatments showing higher emission rates than Control. The temporal pattern mirrored that of α-farnesene, with peak emission rates in the Intermediate treatment occurring between day 26 and day 33 (median ~1.1 × 10^{-3} nmol m^{-2} s^{-1}). Notably, the Severe treatment showed declining emission rates in the last sampling (day 33), consistent with the decrease observed in total sesquiterpene emissions (Fig. 4e). Control plants maintained minimal β-farnesene emission rates

($< 0.5 \times 10^{-3}$ nmol m^{-2} s^{-1}) across all time points, while the Mild groups' emission rates increased throughout the experiment duration to reach their maximum median of 1.25×10^{-3} nmol m^{-2} s^{-1} on day 33.

Fig. 6 shows temporal dynamics emission rates of four sesquiterpene compounds identified by GC–MS on seven sampling days in the *J. communis* experiment (boxplots: treatment distributions, $n = 4$ in the Intermediate drought treatment, $n = 5$ otherwise). All compounds exhibited a strong drought induction. Longifolene dominated the emission rates, reaching 1.0–1.7 $\times 10^{-3}$ nmol m^{-2} s^{-1} in Severe drought plants (Fig. 6a), significantly exceeding Control from day 3 onwards. Longipinene showed similarly strong induction (median 0.5–1.25 $\times 10^{-4}$ nmol m^{-2} s^{-1} in Severe drought; Fig. 6b), while sesquiterpene#2

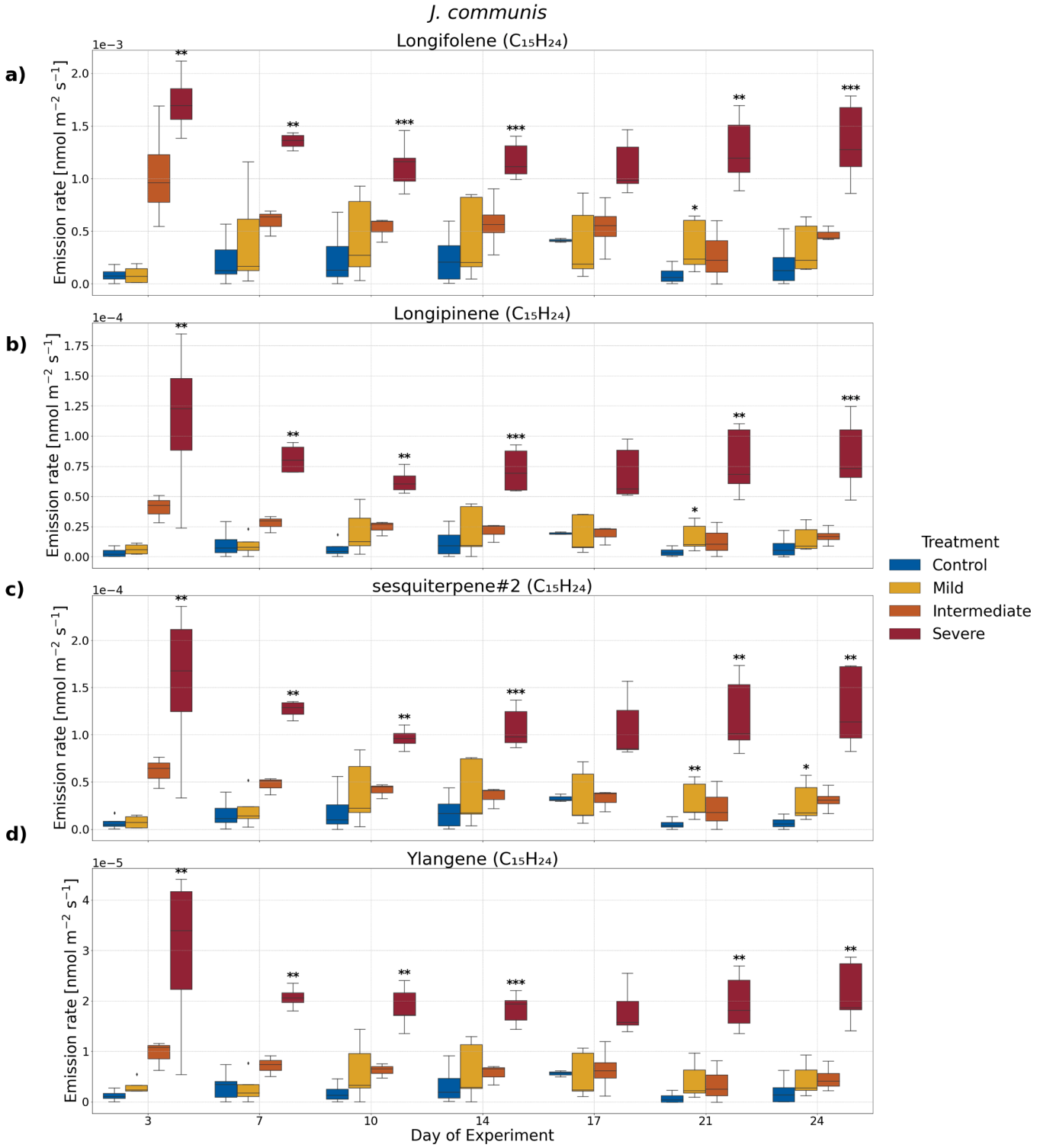

Fig. 6. Mean emission rates of selected BVOCs (including an unidentified sesquiterpene in c) from J. communis in the four treatments, determined for a 7 h light period about every 3rd day with GC–MS. Boxplots represent the median emission rates, the interquartile ranges and whiskers extending to 1.5 times the interquartile range. Please note the different scaling of the *y* axes in the individual panes. Stars indicate significant differences between the drought groups and the control group. Significance levels are: * $p < 0.1$, ** $p < 0.05$, *** $p < 0.01$.

(an unidentified sesquiterpene) and ylangene exhibited parallel patterns at lower absolute rates, still showing significant differences between Control and Severe drought for the whole experiment period (Fig. 6c, d). All four compounds showed immediate elevation in Severe drought from the first sampling (day 3) and sustained high emissions throughout the 27-day experiment, despite near-zero photosynthesis and net carbon loss in these plants (Fig. 1).

3.5. Co-regulation patterns among terpenoid compounds

Correlation analysis of GC–MS emission rates revealed contrasting regulatory patterns between species (Figs. S5–S8). In *P. sylvestris*, monoterpenes showed complex, subgroup-specific correlations (Fig. S5): a "pinene-like" cluster (α-pinene, β-pinene, 3-carene, sabinene; r = 0.71–0.90) was strongly negatively correlated with β-ocimene (r = −0.75 to −0.84), while D-limonene showed near-zero correlations with most compounds (|r| < 0.30). Sesquiterpenes (Fig. S6) similarly formed distinct clusters, with α-farnesene, β-farnesene and related compounds strongly correlated (r = 0.72–0.99), but longifolene negatively correlated (r = −0.53 to −0.70).

In contrast, *J. communis* exhibited remarkably tight coordination within both the monoterpene and sesquiterpene groups (cf. Fig. S7 + S8). All monoterpenes showed strong positive correlations (r = 0.63–0.99), as did most sesquiterpenes (r = 0.82–0.99), indicating coordinated regulation. Exceptions were isoledene and β-caryophyllene, which showed weak correlations with other sesquiterpenes (r = 0.07–0.52), suggesting independent regulation.

4. Discussion

4.1. Physiological responses confirm contrasting drought strategies

Pinus sylvestris maintained high rates of carbon assimilation (Fig. 1a) under Mild drought, at levels comparable to those observed in the Control group. This suggests that for the phenotype used in this experiment, the optimal Θ_v might have been below the soil's field capacity, which was taken as reference for the Control group. Under Intermediate drought, carbon assimilation decreased only slightly, indicating either a moderate tolerance to water deficit or a risk-prone strategy, keeping photosynthesis as high as possible while accepting the consequences of water loss. Under prolonged Severe drought conditions, photosynthetic activity and stomatal conductance rates declined sharply, nevertheless the plants in these treatments still maintained a substantial net carbon gain (Fig. 1a and S3a).

In contrast, *J. communis* exhibited a more pronounced shift in carbon uptake, with significant reductions in cumulative net carbon gain (Fig. 1b) and stomatal conductance (Fig. S3b) already under Mild drought. The high degree of variability in carbon assimilation observed among the plants of this group (cf. Fig. 1b) suggests intraspecific variation in drought tolerance. It remains unclear, though, why this high degree of variability was only observed in this group. One possible explanation is that the Mild drought group passed a water limitation threshold, causing steep changes in the plant's carbon assimilation capabilities. Some plants in this group might have experienced values of Θ_v just above this threshold, while others may have experienced values just below it, resulting in highly variable assimilation rates.

The differences in carbon uptake for both species are also reflected in the methanol emissions (Fig. S4a and b). Methanol is produced by plants as a by-product of cell wall expansion and can thus be seen as a proxy for growth (Fall and Benson, 1996; Vanzo et al., 2015). In our experiment, methanol emissions peaked in the Control and Mild drought group for both species and declined sharply under Severe drought, suggesting very limited growth.

To examine how this difference in carbon gain reflects in the stomatal optimization in both plants, we tested the Medlyn stomatal optimization parameter g_1 (Fig. 2) following Lin et al. (2015).

This revealed distinct patterns in stomatal behavior across the drought gradient for both species. In *P. sylvestris*, well-watered Control plants showed a large g_1 value (4.00) with a poor model fit (R^2 = -0.403). This indicates the absence of a systematic relationship between g_s and the assimilation-VPD term under non-water-limited conditions (cf. Fig. 2). Under Mild drought, model performance increased substantially (R^2 = 0.574) with g_1 = 3.11, suggesting active regulation of stomatal conductance. The stomatal slope parameter g_1 declined progressively with increasing drought severity, indicating a gradual shift towards more conservative water use strategies as Θ_v decreased. The g_1 values under drought conditions reported in Fig. 2a are consistent with published ranges for conifers under water limitation. For example, Lin et al. (2015) reported values of 1.29 for *P. sylvestris* and 2.22 for *Pinus edulis*.

Together, the sustained positive carbon gain alongside the increased stomatal optimization in the Mild to Severe drought groups suggests that *P. sylves*tris exhibits a gradual, continuously regulated response to water limitation. The improved R^2 values under drought (0.496–0.574) compared to Control (−0.403) indicate that the Medlyn model better captures stomatal behavior when water becomes limiting, consistent with the idea that *P. sylvestris* actively optimizes gas exchange under water stress until limitations become sufficiently severe and gas exchange is prohibited (Zweifel et al., 2009).

Juniperus communis exhibited a different response pattern (Fig. 2b). Under Control conditions, we determined a stomatal optimization parameter of g_1 = 4.32, with a poor model fit (R^2 = 0.094), similar to *P. sylvestris*. However, under Mild drought, g_1 remained nearly unchanged at 4.35 despite a negative R^2 value (−0.285), indicating highly variable stomatal behavior with weak optimization. Under Intermediate drought, g_1 declined to 2.31 (R^2 = 0.217), consistent with a shift towards water conservation. Strikingly, under Severe drought, g_1 dropped dramatically to 0.71 (R^2 = 0.465). This extreme reduction in g_1 coincided with near-complete stomatal closure (Fig. S3b) and represents a strongly conservative water use strategy. Overall, our observed g_1 values for *J. communis* under moderate stress are in reasonable agreement with the value of 3.76 reported for the closely related species *Juniperus thurifera* (Lin et al., 2015).

The contrasting patterns between species highlight fundamental differences in drought response strategies. *Pinus sylvestris* showed a gradual, monotonic decline in g_1 across the drought gradient, consistent with progressive stomatal closing. In contrast, *J. communis* maintained relatively high g_1 values under Control and Mild drought (4.32 and 4.35) before undergoing a more abrupt transition to water conservation under Intermediate (2.31) and especially Severe drought (0.71). This pattern suggests that *J. communis* operates with a threshold-based response, maintaining stomata open until a critical stress level triggers strong stomatal closure. This is in line with the observations described in a companion study by de Vries et al. (2026), showing species-specific adaptions for carbonyl sulfide (COS) uptake under different drought levels.

Our results highlight an important limitation of the Medlyn optimization framework: the model is valid within the operational range of stomatal regulation, but fails at the extremes. When plants are not water limited and stomata operate near their maximum conductance without active regulation (Control in both species), the optimization framework breaks down because there is insufficient variation in g_s to model a regulatory response, as was already discussed in other publications (Lin et al., 2015; Duursma et al., 2019). The negative R^2 values under Control and Mild drought conditions indicate that the constrained model (with $g_s$ate that the constrained model (with nd Mild drought conditions indublications (Lin et al., 2015; Duursma et al., 2019). the optimization framework both species under Intermediate and Severe drought) suggest that the Medlyn framework effectively captures stomatal behavior when water becomes limiting and active optimization occurs.

4.2. BVOC Responses to soil water limitation

In the following, we will discuss the results shown above (Section 3) and put our findings in the context of available literature. This will be mainly possible for P. sylvestris, since for J. communis, to the best of our knowledge, only little data on BVOC exchange has been published so far (e.g., Foudil-Cherif et al., 2009; Judzentiene, 2019) and no drought effects on BVOC emissions have been studied.

4.2.1. Monoterpenes: drought-related shifts in single isomer signals are obscured by an invariant bulk monoterpene flux in both species

As illustrated in Figures 3 − 6, *J. communis* generally emits substantially less BVOC per unit area than *P. sylvestris*. Summed monoterpenes measured with PTR-ToF-MS (*m/z* 137.133 + 81.070) showed little systematic dependence on Θ_v (see Fig. 3a, b) in both the *P. sylvestris* and *J. communis* experiment. This is consistent with the idea that substantial parts of the total monoterpene emissions come from storage pools, that are largely governed by physical controls, such as temperature, volatility and diffusion, rather than by instantaneous photosynthetic substrate supply alone (Tingey et al. 1980; Guenther et al., 1991; Niinemets and Reichstein, 2003; Ghirardo et al., 2010; Llusià et al., 2016). This is in line with our second hypothesis, that relies on earlier *P. sylvestris* drought studies reporting inconclusive results on drought duration and drought severity dependent monoterpene emissions (Wu et al., 2015; Lüpke et al., 2017; Kreuzwieser et al., 2021). It reinforces the idea that compositional information of terpenoid compounds is essential for data interpretation and modelling.

GC–MS revealed compound-specific drought effects for *P. sylvestris*, even when in PTR-ToF-MS the sums of isomeric compounds appeared stable: D-limonene emissions were consistently higher in Severe and Intermediate drought than in Control, whereas sabinene tended to show the opposite pattern (see Fig. 5a and 5b). Sabinene emissions (Fig. 5a) decreased towards the end of the experiment, suggesting that sabinene storage pools may be depleted under prolonged drought, or that reduced stomatal conductance limits passive volatilization from resin structures. The contrasting responses between the two monoterpenes are consistent with differing source contributions and compound-specific regulation under drought signaling. These findings highlight that even the emissions of BVOCs deriving from the same synthesis pathway (e.g., Dudareva et al., 2006; Fasbender et al., 2018) can evolve differently under plant drought stress. Compound-specific responses can cancel out at the bulk level, highlighting the value of speciated GC–MS analysis for revealing regulatory mechanisms.

This aligns with recent evidence suggesting that resolving source mechanisms (e.g., via enantiomeric/chiral constraints) can reveal drought-dependent emission pathways that are not apparent from total monoterpene mixing ratios (Byron et al., 2022).

We also observed extraordinarily high levels of monoterpene emissions at the start of the experiment. This is a common observation seen in similar experiments (e.g., Ruuskanen et al., 2005) and is in line with GLV emission peaks (Fig. S4e, f), suggesting mechanical damage, while placing the plants into the cuvettes, to be the main cause. For monoterpenes, this effect was most pronounced in the Severe drought group, so the emissions might not only be related to mechanical damage, but also to a release from storage pools, where reduced elasticity of dry plant matter might have been responsible for the remarkably high emissions from severely drought stressed plants.

4.2.2. Sesquiterpenes: clearest drought indicator with species-specific emission patterns

Both the time-course and the Θ_v-dependency of sesquiterpene emissions were different between the two species. The emission of sesquiterpenes increased towards low Θ_v in both species (see Fig. 3e and 3f), but this effect was stronger and more significant for *J. communis*. For *P. sylvestris,* maximum sesquiterpene emissions occurred at the transition from low to very low Θ_v (5−15 %), suggesting an optimal stress level for induction before severe metabolic limitation sets in.

The time course of sesquiterpene emissions from *P. sylvestris* was complex. The observed drought response behavior—strong emissions under moderate stress, declining with increasing severity or duration—has been reported previously for other BVOCs and other ecosystems (e.g., Seco et al., 2015; Werner et al., 2021). The Severe drought group showed a bell-shaped pattern with highest emission rates halfway through the experiment. The Intermediate drought group also followed this pattern, but with a much larger emission amplitude. Control and Mild groups showed a more linearly rising emission rate, with the Mild group even surpassing the Intermediate group towards the end of the experiment. This implies that the interpretation of sesquiterpene signals in drought experiments cannot rely on Θ_v alone, as acclimation and cumulative stress duration strongly influence emission trajectories. This is consistent with the severity/duration threshold framework for induced BVOCs (Niinemets, 2010), as well as with the evidence that terpene pools and non-foliar sources can contribute dynamically under water stress (Vanhatalo et al., 2020; Rissanen et al., 2022).

The most abundantly emitted sesquiterpenes from *P. sylvestris* during our experiment were α- and β-farnesene. In $^{13}CO_2$ labelling experiments, Kreuzwieser et al. (2021) showed that both are produced de-novo in needles of *P. sylvestris*. A basic role in the synthesis of sesquiterpenes plays pyruvate. Pyruvate is first converted to acetyl-CoA, which then enters the cytosolic MVA pathway. Here, it generates isopentenyl pyrophosphate (IPP) and dimethylallyl pyrophosphate (DMAPP), which condense to form farnesyl pyrophosphate (FPP). FPP is the direct precursor of sesquiterpenes (Oliver et al., 2009; Dudareva et al., 2013). Right after our drought experiment, Stegner et al. (in preparation) conducted a metabolite analysis of the needles from the same sample plants. They found that the pyruvate content was lower in the needles of the Severe drought group of *P. sylvestris* compared to the Control trees, indicating reduced supply of the substrate for the MVA pathway and potential limitations on *de-novo* synthesis. This would argue for a decline in sesquiterpene emissions, as observed by Kreuzwieser et al. (2021) for α- and β-farnesene. In our experiment, however, we observed enhanced sesquiterpene emissions in the drought stressed groups compared to the control group. This was evident in both the PTR-MS an GC–MS measurements. One possible explanation for decreasing pyruvate levels but increasing sesquiterpene emissions could be the existence of not yet identified sesquiterpene pools, which are slowly depleting upon drought stress. Only when these pools are emptied and no more sesquiterpenes can be synthesized due to a lack of the pyruvate substrate, the sesquiterpene emission ceases. In the Severe drought treatment of *P. sylvestris*, we could indeed observe a gradual decrease of sesquiterpene emissions towards the end of the experiment, as part of the bell-shaped pattern described above.

Another explanation for the increased sesquiterpene emissions observed under drought stress could be a specific upregulation of sesquiterpene synthesis overcompensating increasing substrate limitation. Integrated transcriptomic and metabolic analyses of *Atractylodes chinensis* have demonstrated the upregulation of MVA pathway genes and downstream terpene synthases associated with drought, resulting in elevated sesquiterpenoid accumulation under moderate water deficit (Ma et al., 2024). In *Santalum album*, drought upregulates an AREB transcription factor, enhancing the expression of a cytochrome P450 involved in sesquiterpene (santalol) biosynthesis concomitant with increased sesquiterpenoid levels (Meng et al., 2025). These studies support a model in which drought triggers the stress-responsive regulation of biosynthetic pathways, temporarily increasing the metabolic flux towards volatile production, despite the reduced availability of carbon substrates.

Juniperus communis displayed a clear separation of sesquiterpene emission rates between the treatment groups, with highest emission rates in the Severe group, followed by Intermediate, Mild and Control. Notably, the Severe drought group exhibited elevated night-time

emissions (approximately 0.025 nmol m^{-2} s^{-1}), as well as enhanced daytime peaks. This may be related to an increased pool release and/or stress-induced diffusion when stomatal conductance is strongly suppressed. The treatment dependent sesquiterpene release was also confirmed by GC–MS measurements that revealed the same temporal pattern for all measured sesquiterpene compounds. Similar to *P. sylvestris*, also in *J. communis* a metabolic analysis of the needles after our drought experiment showed that the pyruvate content was lower in needles of severely drought stressed than in those of unstressed sample plants (Stegner et al., in preparation). This suggest the release of sesquiterpenes from pre-formed pools that are potentially stored in resin ducts or intracellular compartments. This component becomes more accessible as stomatal conductance declines and membrane permeability increases under stress.

Taken together, our findings in *P. sylvestris* and *J. communis* support a model in which drought enhances sesquiterpene emissions through biosynthetic upregulation and the mobilization of pre-existing pools. Eventually, emissions decline as the substrate pools are depleted under prolonged stress. This pattern is consistent with the growing body of evidence suggesting that plant volatile responses to drought are dynamic and nonlinear (Bonn et al., 2019).

4.2.3. MeSA: Damage related vs. signaling related responses

Methyl salicylate is typically known for its role in plant defense from pathogens and herbivores. It plays an essential role in the plant's systemic acquired resistance and to protect plants from oxidative stress (Singewar et al., 2021). The beneficial effect in alleviating oxidative stress might support the plant's ability to cope with drought stress, which is often accompanied by oxidative stress (Fiella et al., 2007; Hussain et al., 2019).

Our measurements reveal contrasting, species-specific MeSA responses to drought stress: In *P. sylvestris*, MeSA emissions peaked under moderate Θ_v (Figs. 3b and 4b) and reached maximum values of up to ~0.2 nmol m^{-2} s^{-1} at Θ_v ~5–10% (Fig. 3b). This suggests MeSA production is triggered specifically by intermediate water stress, but suppressed when stomatal closure becomes extreme. In the time course of the experiment, the Intermediate drought group showed the highest mean MeSA emissions (up to ~0.15 nmol m^{-2} s^{-1}), followed by Mild, Severe and Control treatments. The bell-shaped temporal emission pattern detected with PTR-ToF-MS is consistent with the observed stress signaling in the case of sesquiterpenes, peaking under moderate stress and diminishing under prolonged severe limitation. Such nonlinear responses to drought are also consistent with broader observations in BVOC research, where mild to moderate stress can enhance the emission of certain compounds, whereas severe or prolonged stress eventually suppresses emission as metabolic capacity and carbon supply decline (Niinemets, 2010).

In *J. communis*, MeSA fluxes were much lower (up to ~0.0015 nmol m^{-2} s^{-1}) and increased with Θ_v (Fig. 3d). Time series data showed the highest MeSA emissions in the Control group and decreasing emissions with increasing drought severity (Fig. 4d). Our measurements indicate that MeSA emissions in *J. communis* are limited by carbon availability and are not triggered, but rather inhibited by water deficit and do not act as an indicator of drought.

Overall, such divergent patterns between *P. sylvestris* and *J. communis* highlight the complexity of BVOC responses, in which drought can stimulate or inhibit emissions, depending on metabolic regulation and/or stomatal conductance (Holopainen and Gershenzon, 2010; Niinemets, 2010).

4.3. Notes on the synthetic pathways of terpenoid compounds

Correlation analyses of GC–MS emission rates (Supplementary Figures S5–S8) showed different regulatory patterns between species. In *P. sylvestris*, monoterpenes and sesquiterpenes showed no consistent covariation. Some compounds were closely coupled while others appeared independently regulated, indicating multiple biosynthetic pathways and emission mechanisms. This is exemplified by opposing drought responses of D-limonene (increased) versus sabinene (decreased).

In contrast, in *J. communis* isomeric monoterpenes and isomeric sesquiterpenes both exhibited strong correlations with each other, suggesting coordinated regulation. An exception to this is isoledene and β-caryophyllene, whose emissions were decoupled from those of any other sesquiterpene (cf. Supplementary Fig. S8).

These patterns indicate that *P. sylvestris* might employ multiple independent regulatory or synthetic pathways, allowing for compound-specific responses (e.g., D-limonene enhancement vs. sabinene suppression under drought). Conversely, juniper could use centralized control resulting in coordinated upregulation of entire biosynthetic pathways under stress.

5. Conclusion

This study tested four hypotheses regarding drought responses in two conifer species, revealing divergent strategies across both carbon-water relations and BVOC emissions. Our first hypothesis (H1) stated that both species would show progressive stomatal closure and declining CO_2 assimilation under drought. This was confirmed, but with critical species-specific differences not initially anticipated. *Pinus sylvestris* employed a riskier strategy, maintaining positive carbon balance even under severe five-week drought through flexible stomatal regulation, while *J. communis* exhibited a conservative strategy with a threshold-based response maintaining relatively open stomata until a critical stress level triggered strong stomatal closure. Under four-week Severe drought, this closure eventually resulted in net carbon loss and progressive metabolic limitation.

Our second hypothesis (H2) regarding monoterpene emissions was confirmed: total emissions remained drought-insensitive in both species, consistent with passive storage-pool release. However, our exploratory GC–MS analysis revealed a compound-specific regulation, with *P. sylvestris* showing slight opposing monoterpene responses that canceled each other in the PTR-ToF-MS sum signals. This might reconcile some of the contradictory findings from previous studies differing in drought duration and severity. In contrast, *J. communis* exhibited no drought related differences in emissions of isomeric monoterpenes, suggesting species-specific differences in biosynthetic regulation.

Rather than the predicted progressive weakening of sesquiterpene emissions (H3), in *P. sylvestris* we observed strong drought induction with a bell-shaped temporal response in Intermediate and Severe drought treatments, peaking mid-experiment. This suggests initial stress-induced up-regulation followed by substrate limitation under prolonged severe stress. *Juniperus communis* showed immediate, sustained elevation throughout the experiment with pronounced nighttime, i.e., storage pool emissions, confirming sesquiterpenes as robust drought indicators but with distinct species-specific signatures.

Methyl salicylate exhibited opposite drought relationships between species. While we hypothesized (H4) species specific patterns according to carbon availability, we did not expect the difference to be this strong. In *P. sylvestris*, MeSA followed a unimodal pattern peaking at intermediate drought, consistent with active stress signaling when metabolic capacity permits. Conversely, *J. communis* showed declining MeSA emissions with increasing drought severity, demonstrating that this species' conservative strategy and earlier carbon limitation preclude stress-induced BVOC synthesis.

Overall, these findings demonstrate that changes in plant BVOC emissions in response to drought are highly species-specific and depend on both carbon balance and metabolic regulation. Our results underscore the need to characterize drought-induced changes in BVOC emissions across a broader range of species, many of which have been poorly studied to date, in order to improve the representation of these emissions in process-based models.

Declaration of generative AI and AI-assisted technologies in the manuscript preparation process

ChatGPT (OpenAI, GPT-4 and GPT-5) was used to assist with code development and text review. All content was reviewed and verified by the authors, who take full responsibility for the publication.

CRediT authorship contribution statement

Judith Schmack: Writing – review & editing, Writing – original draft, Visualization, Validation, Methodology, Investigation, Formal analysis, Data curation, Conceptualization. **Anna de Vries:** Writing – review & editing, Methodology, Investigation, Conceptualization. **Felix Spielmann:** Writing – review & editing, Methodology, Investigation, Conceptualization. **Jörg-Peter Schnitzler:** Writing – review & editing, Methodology, Conceptualization. **Jana Barbro Winkler:** Writing – review & editing, Methodology, Investigation, Conceptualization. **Baris Weber:** Writing – review & editing, Validation, Methodology, Investigation, Conceptualization. **Georg Wohlfahrt:** Writing – review & editing, Visualization, Validation, Methodology, Funding acquisition, Formal analysis, Conceptualization. **Thomas Karl:** Writing – review & editing, Visualization, Validation, Methodology, Funding acquisition, Formal analysis, Conceptualization. **Werner Jud:** Writing – review & editing, Writing – original draft, Visualization, Validation, Methodology, Investigation, Formal analysis, Conceptualization.

Declaration of competing interest

The authors declare that they have no known competing financial interests or personal relationships that could have appeared to influence the work reported in this paper.

Acknowledgments

This research was funded by the Austrian National Science Fund (FWF, doc.funds) through the project “The Future of Mountain Forests: responses to a drier climate” (grant-doi 10.55776/DOC171).

A special thank you goes out to the gardeners of the Botanical Garden in Innsbruck and the technical staff and gardeners at the Helmholtz Center München, Research Unit Environmental Simulation (EUS), for assistance in the preparation and the realization of the VOC-SCREEN experiment (especially Ulrich Junghans and Peter Kary).

We thank Mario Deutschmann from the Institute of Ecology for his help with the measurements of the soil properties.

Moreover, we acknowledge the help of Andreas Osl from Landesforgarten Bad Häring for selecting the plants for the experiment.

Supplementary materials

Supplementary material associated with this article can be found, in the online version, at doi:10.1016/j.stress.2026.101480.

Data availability

Data will be made available on request.

References

Baldwin, I.T., Halitschke, R., Paschold, A., von Dahl, C.C., Preston, C.A., 2006. Volatile signaling in plant-plant interactions: “talking trees” in the genomics era. Science 311 (5762), 812–815. https://doi.org/10.1126/science.1118446.

Bonn, B., Moorgat, G.K., 2002. New particle formation during α- and β-pinene oxidation by O_3, OH and NO_3, and the influence of water vapour: Particle size distribution studies. Atmos. Chem. Phys. 2 (3), 183–196. https://doi.org/10.5194/acp-2-183-2002.

Bonn, B., Magh, R.-K., Rombach, J., Kreuzwieser, J., 2019. Biogenic isoprenoid emissions under drought stress: different responses for isoprene and terpenes. Biogeosciences 16, 4627–4645. https://doi.org/10.5194/bg-16-4627-2019.

Byron, J., Kreuzwieser, J., Purser, G., van Haren, J., Ladd, S.N., Meredith, L.K., Werner, C., Williams, J., 2022. Chiral monoterpenes reveal forest emission mechanisms and drought responses. Nature 609 (7926), 307–312. https://doi.org/10.1038/s41586-022-05020-5.

de Vries, A.de, Spielmann, F., Hammerle, A., Schmack, J., Jud, W., Karl, T., Schnitzler, J.-P., Winkler, J.B., Wohlfahrt, G., 2026. Drought effects on the leaf uptake of carbonyl sulfide and CO_2 in Pinus sylvestris and Juniperus communis. Plant Stress 21, 101355. https://doi.org/10.1016/j.stress.2026.101355.

Dudareva, N., Negre, F., Nagegowda, D.A., Orlova, I., 2006. Plant volatiles: recent advances and future perspectives. Crit. Rev. Plant Sci. 25 (5), 417–440. https://doi.org/10.1080/07352680600899973.

Duan, Y., Lyu, B., Zhang, C., Shi, L., Li, J., Liu, Y., Chen, Q., 2024. Antibacterial activity of the biogenic volatile organic compounds from three species of bamboo. Front. Plant Sci. 15. https://doi.org/10.3389/fpls.2024.1474401.

Dudareva, N., Klempien, A., Muhlemann, J.K., Kaplan, I., 2013. Biosynthesis, function and metabolic engineering of plant volatile organic compounds. New Phytol 198 (1), 16–32. https://doi.org/10.1111/nph.12145.

Dudareva, N., Pichersky, E., 2006. The chemical diversity of floral scent. Biology of Floral Scent. CRC Press, pp. 27–52. https://doi.org/10.1201/9781420004007-2, 1. Aufl., S.

Durrant, T., de Rigo, D., Caudullo, G., 2016. Pinus sylvestris in Europe: distribution, habitat, usage and threats. In: San-Miguel-Ayanz, J., de Rigo, D., Caudullo, G., Houston Durrant, T., Mauri, A. (Eds.), European Atlas of Forest Tree Species. Publ. Off. EU, Luxembourg e016b94+.

Duursma, R.A., Blackman, C.J., Lopéz, R., Martin-StPaul, N.K., Cochard, H., Medlyn, B. E., 2019. On the minimum leaf conductance: its role in models of plant water use, and ecological and environmental controls. New Phytol. 221 (2), 693–705. https://doi.org/10.1111/nph.15395.

Enescu, C.M., Houston Durrant, T., Caudullo, G., de Rigo, D., 2016. Juniperus communis in Europe: distribution, habitat, usage and threats. In: San-Miguel-Ayanz, J., de Rigo, D., Caudullo, G., Houston Durrant, T., Mauri, A. (Eds.), European Atlas of Forest Tree Species. Publ. Off. EU, Luxembourg. E01d2de+.

Fall, R., Benson, A.A., 1996. Leaf methanol—the simplest natural product from plants. Trends Plant Sci. 1 (9), 296–301. https://doi.org/10.1016/s1360-1385(96)88175-0.

Farquhar, G.D., Sharkey, T.D., 1982. Stomatal conductance and photosynthesis. Ann. Rev. Plant Phys. 33 (1), 317–345. https://doi.org/10.1146/annurev.pp.33.060182.001533.

Fasbender, L., Yáñez-Serrano, A.M., Kreuzwieser, J., Dubbert, D., Werner, C., 2018. Real-time carbon allocation into biogenic volatile organic compounds (BVOCs) and respiratory carbon dioxide (CO_2) traced by PTR-TOF-MS, $^{13}CO_2$ laser spectroscopy and ^{13}C-pyruvate labelling. PLoS ONE 13 (9), e0204398. https://doi.org/10.1371/journal.pone.0204398.

Fehsenfeld, F., Calvert, J., Fall, R., Goldan, P., Guenther, A.B., Hewitt, C.N., Lamb, B., Liu, S., Trainer, M., Westberg, H., Zimmerman, P., 1992. Emissions of volatile organic compounds from vegetation and the implications for atmospheric chemistry. Glob. Biogeochem. Cycles 6 (4), 389–430. https://doi.org/10.1029/92gb02125.

Ferracci, V., Bolas, C.G., Freshwater, R.A., Staniaszek, Z., King, T., Jaars, K., Otu-Larbi, F., Beale, J., Malhi, Y., Waine, T.W., Jones, R.L., Ashworth, K., Harris, N.R.P., 2020. Continuous isoprene measurements in a UK temperate forest for a whole growing season: effects of drought stress during the 2018 heatwave. Geophys. Res. Lett. 47 (15), e2020GL088885. https://doi.org/10.1029/2020GL088885.

Filella, I., Wilkinson, M.J., Llusià, J., Hewitt, C.N., Peñuelas, J., 2007. Volatile organic compounds emissions in Norway spruce (*Picea abies*) in response to temperature changes. Physiol. Plant. 130 (1), 58–66. https://doi.org/10.1111/j.1399-3054.2007.00881.x.

Fischler, M.A., Bolles, R.C., 1981. Random sample consensus: a paradigm for model fitting with applications to image analysis and automated cartography. Commun. ACM 24 (6), 381–395. https://doi.org/10.1145/358669.358692.

Fitzky, A.C., Kaser, L., Peron, A., Karl, T., Graus, M., Tholen, D., Halbwirth, H., Trimmel, H., Pesendorfer, M., Rewald, B., Sandén, H., 2023. Same, same, but different: drought and salinity affect BVOC emission rate and alter blend composition of urban trees. Urban For. Urban Green 80, 127842. https://doi.org/10.1016/j.ufug.2023.127842.

Fortunati, A., Barta, C., Brilli, F., Centritto, M., Zimmer, I., Schnitzler, J.-P., Loreto, F., 2008. Isoprene emission is not temperature-dependent during and after severe drought-stress: a physiological and biochemical analysis. Plant J. 55 (4), 687–697. https://doi.org/10.1111/j.1365-313X.2008.03538.x.

Foudil-Cherif, Y., Yassaa, N., Boutarene, N., Meklati, B.Y., 2009. Study of biogenic volatile organic compounds emitted from Juniperus communis and Juniperus oxycedrus growing in Algeria. In: Proceedings of the Global Conference on Global Warming. Istanbul, Turkey.

Ghirardo, A., Koch, K., Taipale, R., Zimmer, I., Schnitzler, J.-P., Rinne, J., 2010. Determination of de novo and pool emissions of terpenes from four common boreal/alpine trees by 13CO2 labelling and PTR-MS analysis. Plant Cell Environ. 33 (5), 781–792. https://doi.org/10.1111/j.1365-3040.2009.02104.x.

Grant, O.M., 2012. Understanding and exploiting the impact of drought stress on plant physiology. In: Ahmad, P., Prasad, M. (Eds.), Abiotic Stress Responses in Plants. Springer, New York, NY. https://doi.org/10.1007/978-1-4614-0634-1_5.

Guenther, A.B., Monson, R.K., Fall, R., 1991. Isoprene and monoterpene emission rate variability: observations with eucalyptus and emission rate algorithm development. J. Geophys. Res. Atmos. 96 (D6), 10799–10808. https://doi.org/10.1029/91JD00960.

Guenther, A., Hewitt, C.N., Erickson, D., Fall, R., Geron, C., Graedel, T., Harley, P., Klinger, L., Lerdau, M., Mckay, W.A., Pierce, T., Scholes, B., Steinbrecher, R., Tallamraju, R., Taylor, J., Zimmerman, P., 1995. A global model of natural volatile

organic compound emissions. J. Geophys. Res. Atmos. 100 (D5), 8873–8892. https://doi.org/10.1029/94JD02950.
Guenther, A.B., Jiang, X., Heald, C.L., Sakulyanontvittaya, T., Duhl, T., Emmons, L.K., Wang, X., 2012. The model of emissions of gases and aerosols from nature version 2.1 (MEGAN2.1): an extended and updated framework for modeling biogenic emissions. Geosci. Model Dev. 5 (6), 1471–1492. https://doi.org/10.5194/gmd-5-1471-2012.
Gupta, A., Rico-Medina, A., Caño-Delgado, A.I., 2020. The physiology of plant responses to drought. Science 368 (6488), 266–269. https://doi.org/10.1126/science.aaz7614.
Holopainen, J.K., Gershenzon, J., 2010. Multiple stress factors and the emission of plant VOCs. Trends Plant Sci. 15 (3), 176–184. https://doi.org/10.1016/j.tplants.2010.01.006.
Hussain, S., Rao, M.J., Anjum, M.A., Ejaz, S., Zakir, I., Ali, M.A., Ahmad, N., Ahmad, S., 2019. Oxidative stress and antioxidant defense in plants under drought conditions. In: Hasanuzzaman, M., Hakeem, K.R., Nahar, K., Alharby, H.F. (Eds.), Plant Abiotic Stress Tolerance: Agronomic, Molecular and Biotechnological Approaches. Springer International Publishing, pp. 207–219. https://doi.org/10.1007/978-3-030-06118-0_9.
Jud, W., Winkler, J.B., Niederbacher, B., Niederbacher, S., Schnitzler, J.-P., 2018. Volatilomics: a non-invasive technique for screening plant phenotypic traits. Plant Methods 14 (1), 109. https://doi.org/10.1186/s13007-018-0378-4.
Judzentiene, A., 2019. Juniperus communis L.: a review of volatile organic compounds of wild and cultivated common juniper in Lithuania. Chemija 30. https://doi.org/10.6001/chemija.v30i3.4053.
Knudsen, J.T., Gershenzon, J., 2020. The chemical diversity of floral scent. In: Pichersky, E., Dudareva, N. (Eds.), Biology of Plant Volatiles, 2nd ed. CRC Press, pp. 57–78. https://doi.org/10.1201/9780429455612-5.
Kotlarski, S., Gobiet, A., Morin, S., Olefs, M., Rajczak, J., Samacoïts, R., 2023. 21st Century alpine climate change. Clim. Dyn. 60 (1), 65–86. https://doi.org/10.1007/s00382-022-06303-3.
Kreuzwieser, J., Meischner, M., Grün, M., Yáñez-Serrano, A.M., Fasbender, L., Werner, C., 2021. Drought affects carbon partitioning into volatile organic compound biosynthesis in Scots pine needles. New Phytol. 232 (5), 1930–1943. https://doi.org/10.1111/nph.17736.
Lin, Y.-S., Medlyn, B., Duursma, R., Prentice, I., Wang, H., Baig, S., Eamus, D., Resco de Dios, V., Mitchell, P., Ellsworth, D., Op de Beeck, M., Wallin, G., Uddling, J., Tarvainen, L., Linderson, M.-L., Cernusak, L., Nippert, J., Ocheltree, T., Tissue, D., Wingate, L., 2015. Optimal stomatal behaviour around the world. Nat. Clim. Change. https://doi.org/10.1038/nclimate2550.
Linton, M.J., Sperry, J.S., Williams, D.G., 1998. Limits to water transport in Juniperus osteosperma and Pinus edulis: Implications for drought tolerance and regulation of transpiration. Funct. Ecol. 12 (6), 906–911. https://doi.org/10.1046/j.1365-2435.1998.00275.x.
Llusia, J., Rohatyn, S., Rotenberg, E., Seco, R., Guenther, A., Penuelas, J., 2016. Photosynthesis, stomatal conductance and terpene emission response to water availability in dry and mesic Mediterranean forests. Trees 30. https://doi.org/10.1007/s00468-015-1317-x.
Loreto, F., Schnitzler, J.-P., 2010. Abiotic stresses and induced BVOCs. Trends Plant Sci. 15 (3), 154–166. https://doi.org/10.1016/j.tplants.2009.12.006.
Lüpke, M., Leuchner, M., Steinbrecher, R., Menzel, A., 2017. Quantification of monoterpene emission sources of a conifer species in response to experimental drought. AoB PLANTS 9 (5). https://doi.org/10.1093/aobpla/plx045.
Ma, S., Sun, C., Su, W., Zhao, W., Zhang, S., Su, S., Xie, B., Kong, L., Zheng, J., 2024. Transcriptomic and physiological analysis of *Atractylodes chinensis* in response to drought stress reveals the putative genes related to sesquiterpenoid biosynthesis. BMC Plant Biol. 24 (1), 91. https://doi.org/10.1186/s12870-024-04780-8.
Medlyn, B.E., Duursma, R.A., Eamus, D., Ellsworth, D.S., Prentice, I.C., Barton, C.V.M., Crous, K.Y., De Angelis, P., Freeman, M., Wingate, L., 2011. Reconciling the optimal and empirical approaches to modelling stomatal conductance. Glob. Chan. Biol. 17 (6), 2134–2144. https://doi.org/10.1111/j.1365-2486.2010.02375.x.
Medlyn, B.E., Duursma, R.A., Eamus, D., Ellsworth, D.S., Colin Prentice, I., Barton, C.V. M., Crous, K.Y., de Angelis, P., Freeman, M., Wingate, L., 2012. Corrigendum to: reconciling the optimal and empirical approaches to modelling stomatal conductance. Glob. Chan. Biol. 18 (11), 3476. https://doi.org/10.1111/j.1365-2486.2012.02790.x.
Meng, S., Lian, N., Qin, F., Yang, S., Meng, D., Bian, Z., Xiang, L., Lu, J., 2025. The AREB transcription factor *SaAREB6* promotes drought stressinduced santalol biosynthesis in sandalwood. Horticult. Res. 12 (3), 347. https://doi.org/10.1093/hr/uhae347.
Muller, J.D., Rotenberg, E., Tatarinov, F., Oz, I., Yakir, D., 2021. Evidence for efficient nonevaporative leaf-to-air heat dissipation in a pine forest under drought conditions. New Phytol 232 (6), 2254–2266. https://doi.org/10.1111/nph.17742.
Nabeta, K., Kawakita, K., Yada, Y., Okuyama, H., 1993. Biosynthesis of sesquiterpenes from deuterated mevalonates in Perilla Callus. Biosci. Biotechnol. Biochem. 57 (5), 792–798. https://doi.org/10.1271/bbb.57.792.
Niinemets, Ü., 2010. Mild versus severe stress and BVOCs: Thresholds, priming and consequences. Trends Plant Sci. 15 (3), 145–153. https://doi.org/10.1016/j.tplants.2009.11.008.
Niinemets, Ü., Reichstein, M., 2003. Controls on the emission of plant volatiles through stomata: differential sensitivity of emission rates to stomatal closure explained. J. Geophys. Res. Atmos. 108 (D7), 2002JD002620. https://doi.org/10.1029/2002JD002620.
Oliver, D.J., Nikolau, B.J., Wurtele, E.S., 2009. Acetyl-CoA—life at the metabolic nexus. Plant Sci 176 (5), 597–601. https://doi.org/10.1016/j.plantsci.2009.02.005.
Peñuelas, J., Staudt, M., 2010. BVOCs and global change. Trends Plant Sci. 15 (3), 133–144. https://doi.org/10.1016/j.tplants.2009.12.005.
Pichersky, E., Noel, J.P., Dudareva, N., 2006. Biosynthesis of plant volatiles: nature's diversity and ingenuity. Science 311 (5762), 808–811. https://doi.org/10.1126/science.1118510.
Platter, A., Scholz, K., Hammerle, A., Rotach, M.W., Wohlfahrt, G., 2024. Agreement of multiple night- and daytime filtering approaches of eddy covariance-derived net ecosystem CO 2 exchange over a mountain forest. Agric. For. Meteor. 356, 110173. https://doi.org/10.1016/j.agrformet.2024.110173.
Rissanen, K., Aalto, J., Gessler, A., Hölttä, T., Rigling, A., Schaub, M., Bäck, J., 2022. Drought effects on volatile organic compound emissions from Scots pine stems. Plant Cell Environ. 45 (1), 23–40. https://doi.org/10.1111/pce.14219.
Roy, J., Rineau, F., De Boeck, H.J., Nijs, I., Pütz, T., Abiven, S., Arnone III, J.A., Barton, C. V.M., Beenaerts, N., Brüggemann, N., Dainese, M., Domisch, T., Eisenhauer, N., Garré, S., Gebler, A., Ghirardo, A., Jasoni, R.L., Kowalchuk, G., Landais, D., Milcu, A., 2021. Ecotrons: powerful and versatile ecosystem analysers for ecology, agronomy and environmental science. Glob. Chang. Biol. 27 (7), 1387–1407. https://doi.org/10.1111/gcb.15471.
Ruuskanen, T.M., Kolari, P., Bäck, J., Kulmala, M., Rinne, J., Hakola, H., Taipale, R., Raivonen, M., Altimir, N., Hari, P., 2005. On-line field measurements of monoterpene emissions from Scots pine by proton-transfer-reaction mass spectrometry. Boreal Environ. Res. 10 (6), 553–567.
Sancho-Knapik, D., Sanz, M.Á., Peguero-Pina, J.J., Niinemets, Ü., Gil-Pelegrín, E., 2017. Changes of secondary metabolites in Pinus sylvestris L. needles under increasing soil water deficit. Ann. For. Sci. 74 (1), 24. https://doi.org/10.1007/s13595-017-0620-7.
Seco, R., Karl, T., Guenther, A., Hosman, K.P., Pallardy, S.G., Gu, L., Geron, C., Harley, P., Kim, S., 2015. Ecosystem-scale volatile organic compound fluxes during an extreme drought in a broadleaf temperate forest of the Missouri Ozarks (central USA). Glob. Chang. Biol. 21 (10), 3657–3674. https://doi.org/10.1111/gcb.12980.
Seidel, H., Schunk, C., Matiu, M., Menzel, A., 2016. Diverging drought resistance of scots pine provenances revealed by infrared thermography. Frontiers Plant Sci. 7. https://doi.org/10.3389/fpls.2016.01247.
Singewar, K., Fladung, M., Robischon, M., 2021. Methyl salicylate as a signaling compound that contributes to forest ecosystem stability. Trees 35 (6), 1755–1769. https://doi.org/10.1007/s00468-021-02191-y.
Tetens, O., 1930. Über einige meteorologische Begriffe. Z. Geophys. 6, 297–309.
Tingey, D.T., Manning, M., Grothaus, L.C., Burns, W.F., 1980. Influence of light and temperature on monoterpene emission rates from slash Pine. Plant Physiol. 65 (5), 797–801. https://doi.org/10.1104/pp.65.5.797.
Vanhatalo, A., Aalto, J., Chan, T., Hölttä, T., Kolari, P., Rissanen, K., Kabiri, K., Hellén, H., Bäck, J., 2020. Scots pine stems as dynamic sources of monoterpene and methanol emissions. Frontiers For. Glob. Chang. 2. https://doi.org/10.3389/ffgc.2019.00095.
Vanzo, E., Jud, W., Li, Z., Albert, A., Domagalska, M.A., Ghirardo, A., Niederbacher, B., Frenzel, J., Beemster, G.T.S., Asard, H., Rennenberg, H., Sharkey, T.D., Hansel, A., Schnitzler, J.-P., 2015. Facing the future: effects of short-term climate extremes on isoprene-emitting and non-emitting poplar. Plant Physiol. 169 (1), 560–575. https://doi.org/10.1104/pp.15.00871.
von Caemmerer, S., Farquhar, G.D., 1981. Some relationships between the biochemistry of photosynthesis and the gas exchange of leaves. Planta 153 (4), 376–387. https://doi.org/10.1007/BF00384257.
Weber, P., Bugmann, H., Rigling, A., 2007. Radial growth responses to drought of Pinus sylvestris and Quercus pubescens in an inner-Alpine dry valley. J.Veg. Sci. 18 (6), 777–792. https://doi.org/10.1111/j.1654-1103.2007.tb02594.x.
Werner, C., Meredith, L.K., Ladd, S.N., Ingrisch, J., Kübert, A., Van Haren, J., Bahn, M., Bailey, K., Bamberger, I., Beyer, M., Blomdahl, D., Byron, J., Daber, E., Deleeuw, J., Dippold, M.A., Fudyma, J., Gil-Loaiza, J., Honeker, L.K., Hu, J., Williams, J., 2021. Ecosystem fluxes during drought and recovery in an experimental forest. Science 374 (6574), 1514–1518. https://doi.org/10.1126/science.abj6789.
Wu, C., Pullinen, I., Andres, S., Carriero, G., Fares, S., Goldbach, H., Hacker, L., Kasal, T., Kiendler-Scharr, A., Kleist, E., Paoletti, E., Wahner, A., Wildt, J., Mentel, Th.F., 2015. Impacts of soil moisture on de-novo monoterpene emissions from European beech, Holm oak, Scots pine, and Norway spruce. Biogeosciences 12 (1), 177–191. https://doi.org/10.5194/bg-12-177-2015.
Zweifel, R., Rigling, A., Dobbertin, M., 2009. Species-specific stomatal response of trees to drought – a link to vegetation dynamics? J. Veg. Sci. 20 (3), 442–454. https://doi.org/10.1111/j.1654-1103.2009.05701.x.